Doctoral Dissertation

Studies on metal-containing chemically amplified resist utilizing polarity change and crosslinking for extreme ultraviolet lithography

（極端紫外光リソグラフィに用いる極性変換と架橋を利用した

金属含有化学増幅型レジストに関する研究）

Satoshi Enomoto

Department of Applied Chemistry
Graduate School of Engineering
Osaka University

Preface

The investigation described in this thesis was performed under guidance of Professor Takahiro Kozawa at the Institute of Scientific and Industrial Research, Osaka University.

The objectives of this research are to develop a chemically amplified extreme ultraviolet (EUV) resist with a low acid blur and to clarify the reaction mechanisms of highly EUV-absorbing organo-metal compound incorporated into a chemically amplified resist. The feature of the new negative type resist is the incorporation of several reactive compounds which react as a dissolution changer by hydrophobizing reaction and/or radical recombination. This new chemically amplified negative resists using organo-metal compound as a diffusion control agent was capable of fabricating low LWR pattern with the comparable sensitivity of conventional chemically amplified resist.

Contents

Chapter III
Incorporation of chemical amplification in dual insolubilization resist

General introduction

Mobile devices such as smartphone, tablet device, and personal computers which utilize internet connection have become essential goods in our daily life owing to remarkable development of information technology (IT). The development of IT has been accelerated in various industrial fields for adjusting their service to mobile device platform. For example, all of home appliances will utilize internet connection and will be controlled from outside the home. Such a network is called Internet of Things (IoT). As another example in the financial industry, many securities companies and financial agencies have been corroborating with IT's one to provide innovative services in financial field by introducing IT, which is called Fintech. Coupled with that, higher integration of microprocessors and memories has progressed to meet a strong demand of technical advancement and downsizing of the devices. Semiconductor devices have been mass-produced using the photolithography process. Electrodes of a semiconductor chip are fabricated by repeating etching, oxidation, diffusion, chemical vaper deposition (CVD), and ion implantation to the pattern formed on the silicon substrate by photolithography utilizing a photosensitive imaging material called photoresist. Then, the chips are wire-bonded and sealed to form semiconductor devices.

The development of high integration of semiconductors has progressed based on the empirical rule called Moore's law announced in 1965 by Gordon Moore who is a co-founder of Intel Corporation. It stated that semiconductor density will double every 18 months. Nowadays, the numbers of transistors are over 1 billion per chip of large-scale integration (LSI) and technologies to form a pattern size of 15 nm or less have been actively investigated for building higher integration semiconductor. The resolution of the pattern transferred to wafer by the photolithography method can be calculated by the Rayleigh equation shown below.

$$\text{Resolution [nm]} = k_1 \times \lambda / NA \qquad (1)$$

(k_1:Process factor　λ：wavelength [nm]　NA：Numerical aperture)

According to the above formula, the exposure wavelength has been shortened for obtaining a high-resolution pattern, and the shortening of the wavelength is advanced from g-line (436 nm) to i-line (365 nm), KrF excimer laser (248 nm), and ArF excimer laser (193 nm).

Current advanced semiconductor circuits have been fabricated by an immersion ArF (iArF) lithography method, the exposure wavelength of which is decreased to 134 nm, using water (refractive index: 1.44 at the wavelength of 193 nm) with chemically amplified resists (CARs).

CARs are mainly composed of acid reactive polymer, photoacid generator (PAG), and acid quencher such as trialkylamine. The properties of an exposed area are changed by the acid catalytic thermal reaction. The acids are generated from PAG which is a minor component of the resist by absorbing light transferred through a photomask in which a circuit pattern is drawn (Scheme 1 (a)). As the chemical structure of molecules in the exposed area changes, a difference in solubility between the exposed area and the unexposed area arises, and the pattern on the photomask is transferred to the silicon wafer by developing with an organic or aqueous developer (Scheme 1 (c)). The generated acid in CARs is thermally diffused to decompose the acid-reactive protecting group bound to the polymer by a catalytic reaction. Thereby, the number of the decomposition of the protecting groups is larger than that of the acids generated through exposure (Scheme 1 (b-1)). It is, however, required to control the acid diffusion through the acid deactivation at a constant rate by an acid quencher for suppressing the acid catalytic reaction in the unexposed area in order to maintain the pattern shape (Scheme 1(b-2)). By combining these reactions, CARs are capable to generate high dissolution contrast with low exposure dose for making a lithographic pattern, as shown in Fig.1.

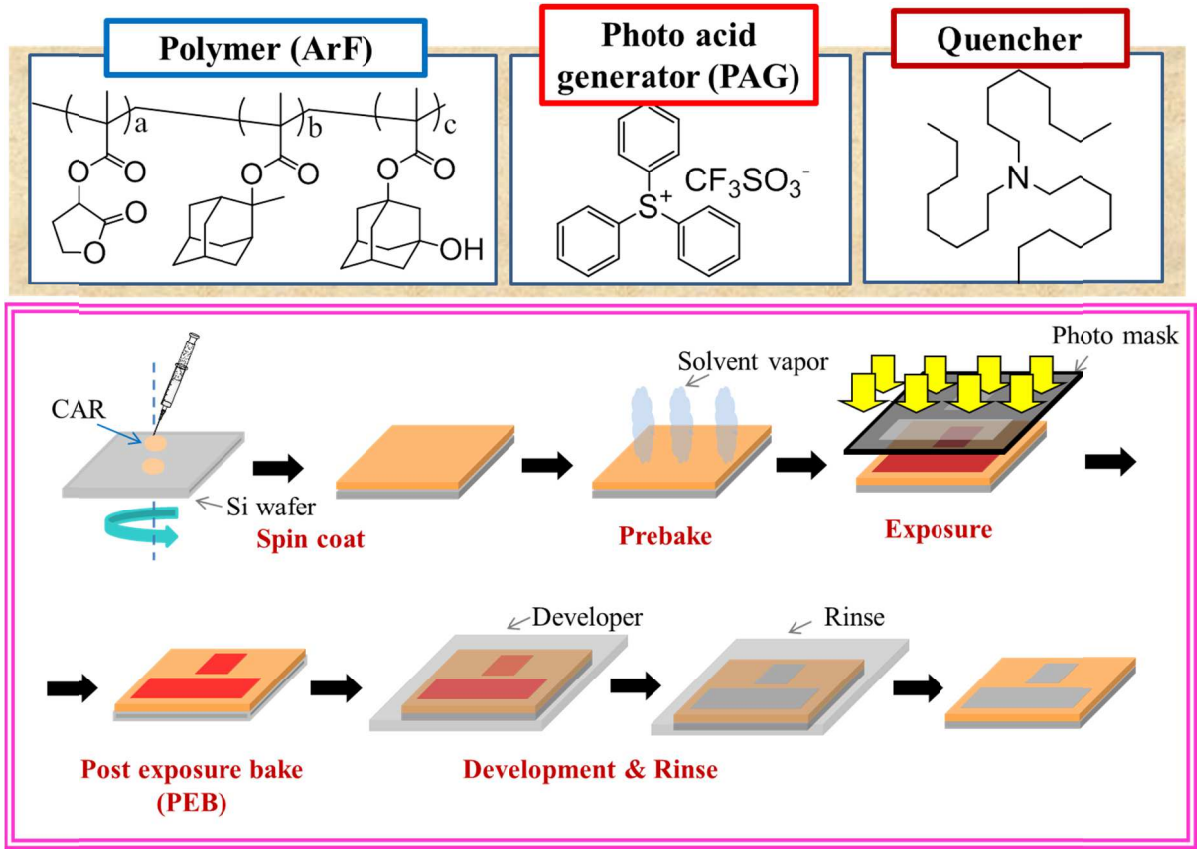

Fig. 1 ArF resist components and photolithography process using CARs.

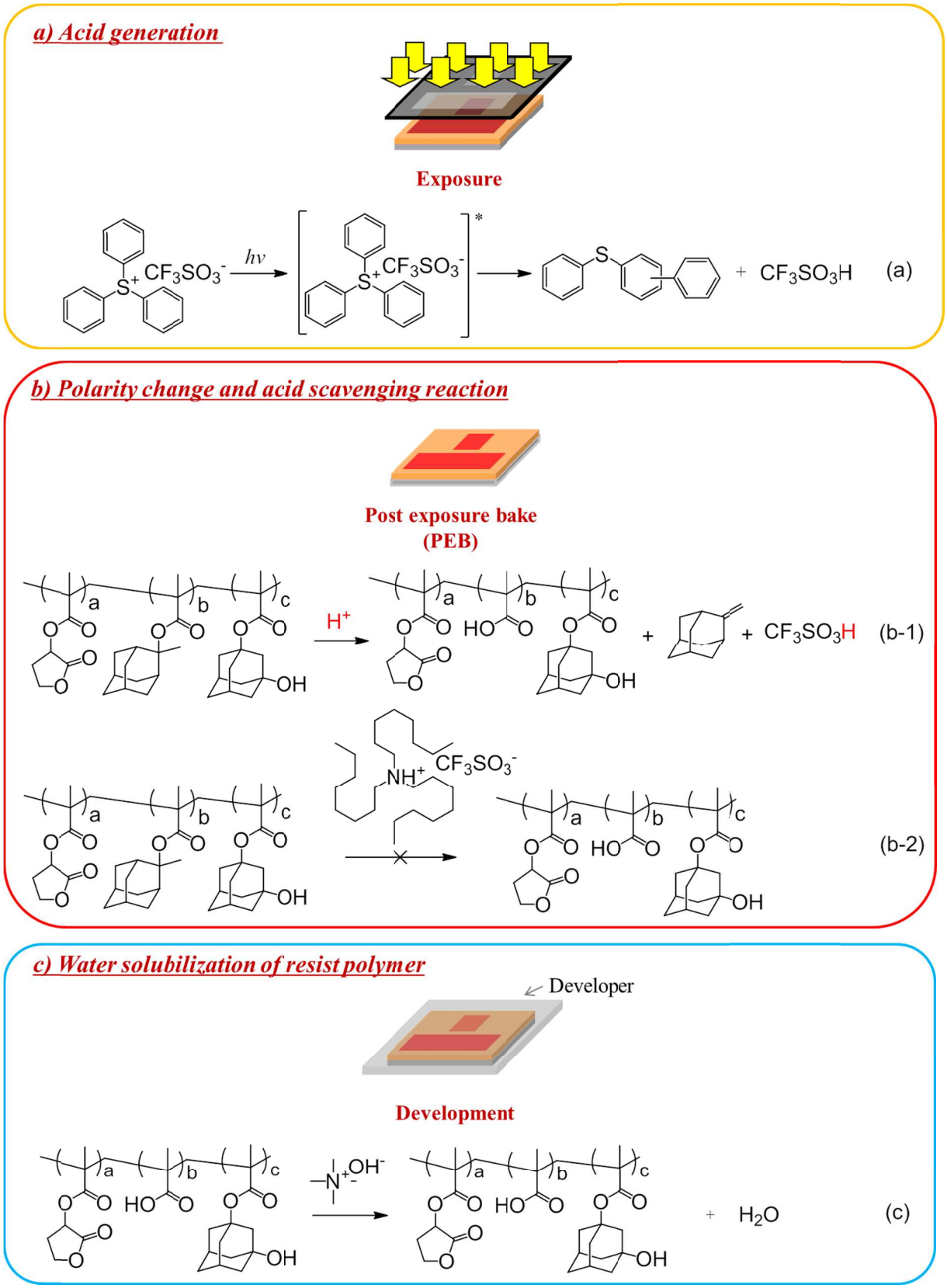

Scheme 1 Details of the reaction in lithography process: (a) acid generation, (b-1) deprotection reaction, (b-2) acid scavenging reaction, (c) hydrophilic reaction

Lithography miniaturization has been advanced according to the International roadmap for device and systems (IRDS). Currently, the resolution of line and space pattern (L/S) is required to be less than 15 nm (half pitch (HP)). However, since 15 nm HP patterning is unachievable in principle at an exposure wavelength of 193 nm, multiple exposures or pitch division by etching have been adopted to produce a pattern[1,2]. The multi-patterning method is an effective technique for improving the resolution, but the number of exposures is extremely large in order to form a complex circuit pattern used in logic devices such as graphics processing unit (GPU), central processing unit (CPU), and the like. Since a mask is required for each exposure, many masks are necessary for making a required pattern, and the circuit pattern designs are limited. Because of such a situation, next lithography technique is required to make a complicated pattern through a single exposure, using a short wavelength light source, and a lithography method using extreme ultraviolet (EUV) at 13.5 nm has been studied as a next-generation light source that replaces an ArF excimer laser (Fig. 2). According to the IRDS lithography roadmap 2017[3], high volume manufacturing (HVM) of semiconductor devices using EUV light source is anticipated because of a high potentially lithography technology that will have been utilized until the end of the size miniaturization of current silicon based semiconductors (Fig.3).

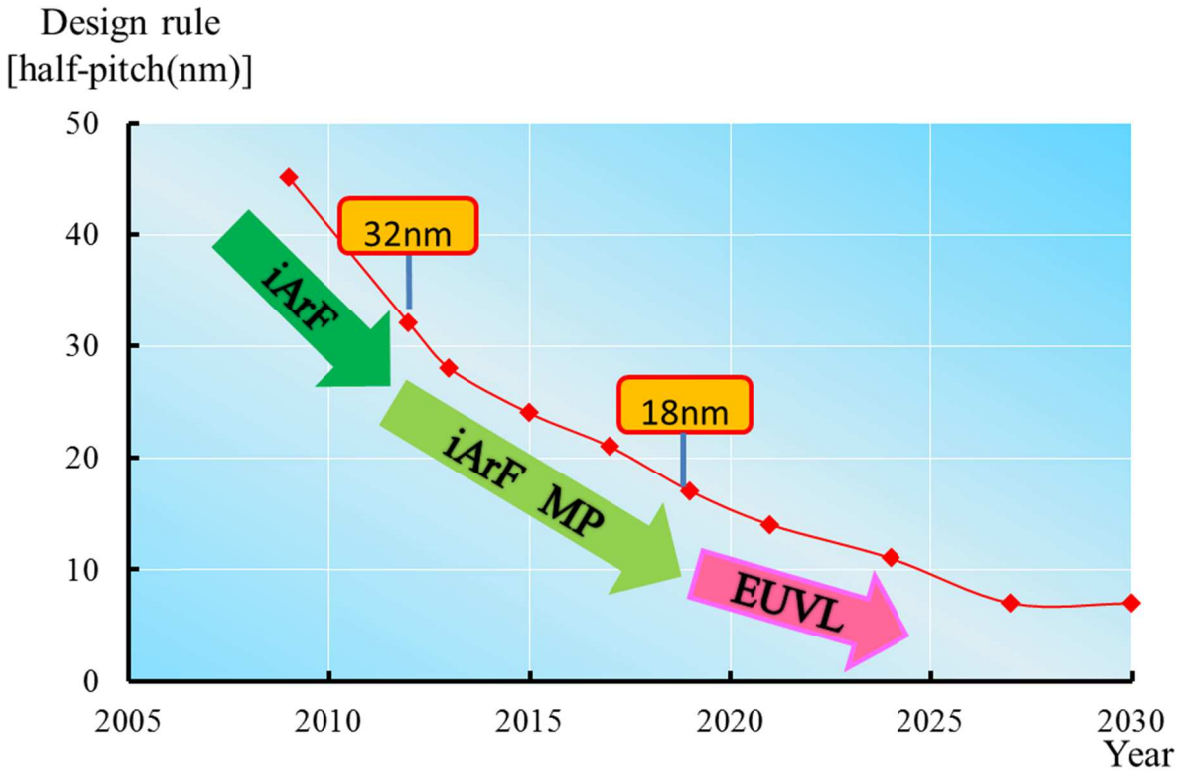

Fig. 2 Lithography roadmap about MPU and DRAM.

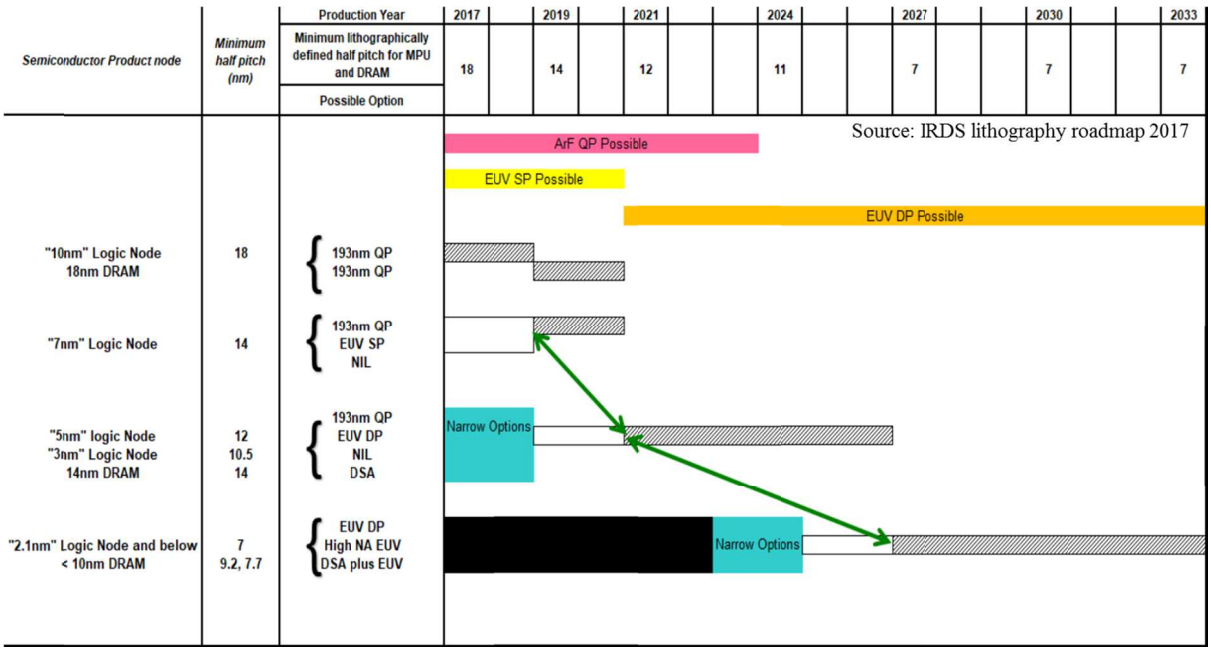

Abbreviations : SP (single patterning), DP (double patterning), QP (quadruple patterning), NIL (nano imprint lithography) DSA (directed self-assembly), MPU (microprocessor unit), DRAM (dynamic random access memory)

Fig. 3 Line and space potential solutions for MPU and DRAM.

As shown in the formula (1), the resolution can be greatly improved by setting the exposure light source to EUV owing to approximately 1/14 of the wavelength of ArF. Therefore, EUV lithography has been avidly developed as a successor of ArF immersion multi-patterning lithography for manufacturing sub-15 nm HP node devices and beyond.[4,5] The patterning with a half-pitch less than 15 nm has been demonstrated using a commercially available EUV exposure tool (ASML NXE:3300) with CARs for the HVM of semiconductor devices.[6,7] However, the performance of CARs has been expected to approach their limitation.[8,9] There is a trade-off relationship between resolution, line width roughness (LWR), and sensitivity (RLS trade-off). The RLS trade-off problems have come to a head with the progress of pattern miniaturization.[10-13] The improvement of LWR and sensitivity without degrading the resolution is technically difficult because of acid diffusion and stochastic effect.[14,15] Stochastic effect is enhanced when the photon energy increased. There is the relationship shown in formula (2) between the photon energy and wavelength of light source.

$$\text{Photon energy } (E)\ [\text{eV}] = hc/\lambda \qquad (2)$$

(h : Planck's constant [eV·s] c : velocity of light in vacuum [m·s]

λ: wavelength [nm])

Since the number of photons from EUV per unit energy decreases to approximately 1/14 as compared to ArF, the density of acid molecules in the exposed area of the resist is decreased. Using the acid diffusion reaction generated by low photon density, it is difficult to obtain a latent image faithful to the mask pattern due to line width roughness (LWR) and line edge roughness (LER) deterioration. In principle, the shot noise effect can be reduced when a large amount of exposure energy is given to the resist. However, the output of the EUV exposure light source is not sufficient for mass production of devices. Therefore, the improvement of the resist sensitivity and the reduction of the LWR are necessary to obtain the sub 15 nm pattern by EUV lithography with consideration for the productivity. To increase sensitivity of the EUV resist, it must be considered that the reaction mechanism of resist by EUV irradiation is greatly different from the conventional photolithography. The photon energy of EUV which is 92.5 eV as shown by the formula (2) greatly exceeds the ionization energy of the organic molecules (approximately 8-10 eV) consisting the CARs. Therefore, the energy deposition of EUV is mainly considered to be caused by the ionization of resist components. It causes the necessity of changing the molecular design concept from g-line to ArF which were focused on the molar absorption coefficient of PAG in regard to the irradiation wavelength (Fig. 4).

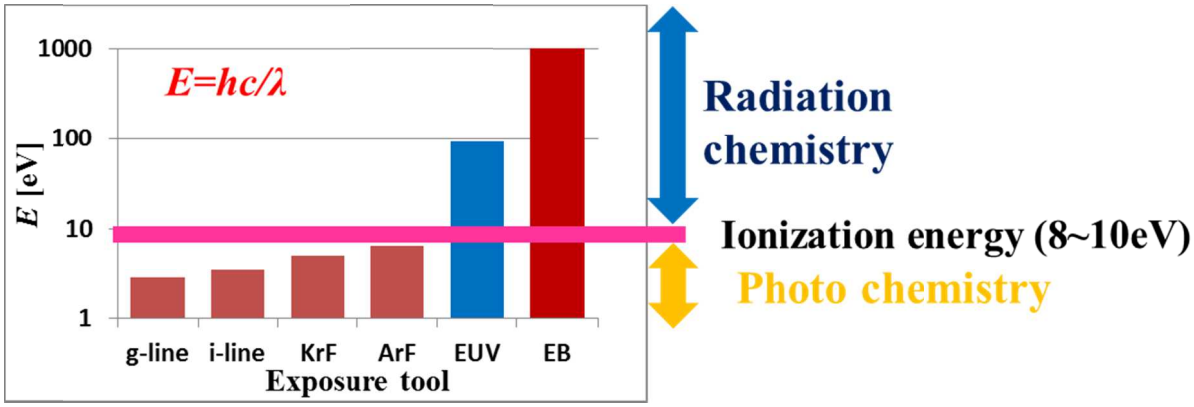

Fig. 4 Photon energy of Exposure tools.

The acid of the chemically amplified resist upon the EUV irradiation is generated by the dissociative electron attachment reaction with thermalized electron. The thermalized electron is generated through the energy loss of the high energy secondary electron which is generated by the ionization of the resist upon the absorption of EUV light. Secondary, an electron can ionize or excite other molecules in the resist when the energy of electron is higher than the ionization potential of resist components (Scheme 2 (1)). An electron with the energy lower than the ionization energy decomposes the cation structure of a PAG by a dissociative electron attachment that reduces the PAG with high electron affinity (Scheme 2 (3)). An anion is

combined with a proton generated through the deprotonation from the radical cation structure of the ionized resist components (Scheme 2 (2), (4)), (Fig.5).

RH ⚡ RH*, $RH^{\bullet+}$, e^-	(Ionization and Excitation)	(1)
$RH^{\bullet+}$ + RH → RH (H)$^+$ + $R^{\cdot}$	(Deprotonation of Polymer Cation radical)	(2)
$Ph_3S^+X^-$ + e^- → Ph_2S + $Ph^{\cdot}$ + X^-	(Electron Scavenging By Acid Generator)	(3)
RH(H)$^+$ + X^- → RH + HX	(Acid Formation)	(4)

Scheme 2 Reaction mechanism of EUV and EB resists through ionization.

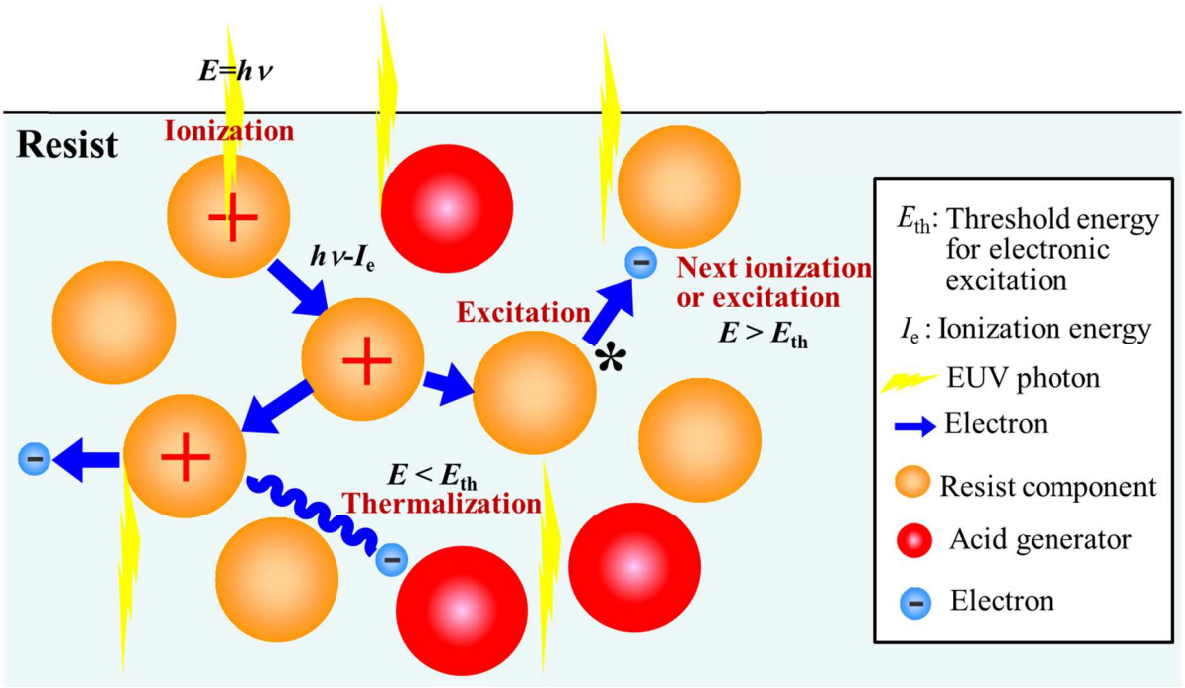

Fig. 5 Acid generation mechanism of CARs by EUV irradiation.

EUV absorption is determined by the sum of atomic absorption of the resist compositions. Thus, the high-density incorporation of high EUV-absorbing atoms is preferable for absorption improvement. However, the EUV absorptivities of main component of conventional CARs such as carbon, hydrogen, and sulfur are low except for oxygen. The examples of atoms with high EUV absorption are fluorine and iodine among halogens, and hafnium, tin, tellurium, and antimony among transition elements (Fig.6).

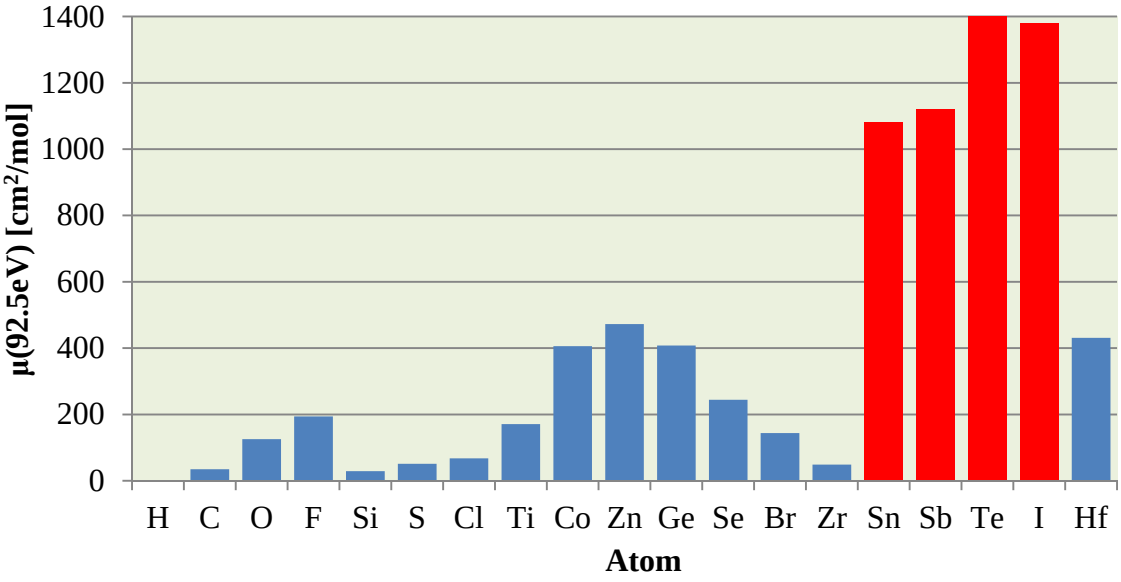

Fig. 6 EUV absorption cross section of major components of CARs and high absorption atoms.

In the past, a fluorine-atom-containing resist, which is easily introduced into CARs, was examined as an EUV resist. However, fluoride anions were eliminated by EUV irradiation or dissociative electron attachment, and the anions recombined with protons to generate hydrofluoric acid. There is a problem that the acid generation from PAG is inhibited.[16,17] Recently, the incorporation of metal compounds in the resist formula has attracted much attention as a mean of increasing the EUV photon absorption efficiency. Some of the novel platforms such as metal nanoparticle resists, molecular organic metal resists, and metal oxo-hydroxo cluster resists have larger EUV photon absorption cross section than CARs. These resists generate dissolution contrast by sol-gel reaction or polymerization using active spices generated upon EUV absorption.[18-20] However, systematic developments of these resists are difficult because their mechanisms of solubility change are still poorly understood. Furthermore, even with a metal containing resists, LWR have not been sufficiently reduced yet, compared with CARs.[21] Non-chemically amplified organic resists (non-CARs) are cited as resists compatible with high resolution and low LWR, and are used for electron beam resists requiring high pattern dimensional accuracy. However, these resists are lowly sensitive to radiations because they do not use any amplification mechanisms like CARs. In order to make a high sensitivity and low LWR EUV resist platform, it is necessary to minimize the influence of shot noise using active species generated from high EUV absorption coefficient components of resist. Utilizing the amplification reaction, the acid diffusion of which is more strictly controlled than the conventional chemically amplification, is also an essential technique to achieve the

sufficient sensitivity for HVM. For that purpose, the knowledge of reactivity of the metal compound incorporated into the organic resists is useful to make a resist design. Therefore, I decided to incorporate reactions that have dissolution contrast by effectively utilizing active species generated by EUV into a resist. I aimed to find a way to improve the sensitivity and further clarify the reaction mechanism by incorporating a metal compound, which has a high EUV absorption cross section, into this resist. In addition to that, I also aimed to construct a highly sensitive EUV resist platform with a small LWR by tightly controlling the diffusion on the basis of the acquired knowledge on the reactivity of metal compounds.

In this study, as a method to make a dissolution contrast to developer with less reaction, sulfonium salt, which is an ionic compound utilized as an acid generator in chemically amplified resist, was bonded to polymer. The sulfonium salt is decomposed to aryl sulfides by the reductive reaction when a secondary electron was generated in the polymer upon EUV irradiation. This reaction generates a large polarity conversion by changing the ionic compound to a nonionic compound. Further, a compound, which generates radicals with the triplet excitation state upon EUV irradiation, is bonded to the same polymer to combine a crosslinking reaction by the radical recombination at the same time. As a result, it was possible to develop an EUV resist with high sensitivity without chemically amplified reaction due to the synergistic effect of the two reactions (Chapter I).

Subsequently, a tin compound having a high EUV absorption coefficient was introduced to the resist polymer described in Chapter I. As a result, the sensitivity became high due to an increase in the EUV absorption coefficient and film density. Furthermore, knowledge about reaction mechanism of tin compound in the resist was obtained by reactivity analysis using EUV and 75keV electron beam (EB) (Chapter II).

In addition, I focused on the reaction mechanisms that a strong acid is generated in the decomposition of the polymer bound sulfonium salt and that the tin compound is utilized as an acid diffusion control agent by reacting with a strong acid below room temperature. By using this reactivity, I introduced a compound that crosslinks by a bimolecular reaction in the presence of an acid catalyst, which is advantageous for the diffusion control, compared with the deprotection reaction as shown in scheme 1 (b-1). As a result, the sensitivity of the polymer was 2.4 times higher than the polymer described in Chapter II. Furthermore, this new chemically amplified negative resists using a metal compound as a diffusion control agent was capable of fabricating a low LWR pattern with similar sensitivity of conventional CARs (Chapter III).

References

1) M. Hori, T. Nagai, and A. Nakamura et al. Proc. SPIE **6923**, 69230H (2008).

2) I. Bouchoms, A. Engelen, and J. Mulkens et al. Proc. SPIE **7274**, 72741K (2009).

3) https://irds.ieee.org/images/files/pdf/2017/2017IRDS_LITH.pdf

4) H. Kinoshita, K. Kurihara, and Y. Ishii et al. J. Vac. Sci. Technol. B **7**, 1648 (1989).

5) M. Kerkhof, H. Jasper, and L. Levasier et al. Proc. SPIE **10143**, 101430D (2017).

6) H. Tsubaki, W. Nihashi, and T. Tsuchihashi et al. Proc. SPIE **9776**, 977608 (2016).

7) T. Fujii, S. Matsumaru, and T. Yamada et al. Proc. SPIE **9776**, 97760Y (2016).

8) T. Kozawa, J. J. Santillan, and T. Itani, Jpn. J. Appl. Phys. **53**, 106501 (2014).

9) T. Kozawa, J. J. Santillan, and T. Itani, Jpn. J. Appl. Phys. **54**, 036507 (2015).

10) G. M. Gallatin, Proc. SPIE **5754**, 38 (2005).

11) D. V. Steenwinckel, R. Gronheid, and J. H. Lammers et al. Micro/Nanolithography MEMS MOEMS **7**, 023002 (2008).

12) P. P. Naulleau, C. N. Anderson, and L. Bacleaan et al. Proc. SPIE **7972**, 797202 (2011).

13) T. Wallow, D. Civay, and S. Wang et al. Proc. SPIE **8322**, 83221J (2012).

14) S. Wurm, Jpn. J. Appl. Phys. **46**, 6105 (2007).

15) A. M. Goethals, P. Foubert, and K. Hosokawa et al. J. Photopolym. Sci. Technol. **25**, 559 (2012).

16) S. Higashino, A. Saeki, and K. Okamoto et al. J. Phys. Chem. A **114**, 8069 (2010).

17) K. Okamoto, N. Nomura, and R. Fujiyoshi et al. J. Phys. Chem. A **121**, 9458 (2017).

18) J. Passarelli, M. Murphy, and R. D. Re, M. Sortland, et al. Proc. SPIE **9425**, 94250T (2015).

19) T. Fujimori, T. Tsuchihashi, and S. Minegishi et al. Proc. SPIE **9776**, 977605 (2016).

20) M. Yu, E. P. Giannelis, and C. K. Ober, Proc. SPIE **9779**, 977905 (2016).

21) A. Pirati, J. Schoot, and J. Troost et.al, Proc. SPIE **10143** 101430G (2017).

Chapter I

Study of electron beam and extreme ultraviolet resist utilizing polarity change and radical crosslinking

1.1 Introduction

Pattern defects due to stochastic effects markedly increase at a half-pitch of less than 15 nm because of the stochastic effect of the acid diffusive chemical reaction of CARs. [1)] Thereby, the development of a novel platform without acid diffusion becomes important. However, the enhancement of sensitivity is a critical issue, because the light source power is currently limited. In conventional non-CARs, the ionization and electronic excitation are generally used for inducing the main-chain scission or crosslinking of molecules, which results in the solubility change of the resist. Although the energy of thermalized electrons is approximately 30 meV, they can be still used for the pattern formation. The acid generation of CARs through EUV/EB exposure is a typical example of the use of thermalized electrons.[2)] The PAGs are decomposed by the dissociative electron attachment to produce the anions of acids and diaryl sulfides when the PAGs are utilized triaryl sulfonium salts. Since this polarity change significantly affects the solubility of the resist in the developer, a sulfonium cation-bounded resist was suggested as a highly sensitive non-CAR, compared to conventional resists such as AR-N 7500[3)] and hydrogen silsesquioxane (HSQ)[4)]. Also, it showed lower line edge roughness (LER) than CARs.[5)]

For the sensitivity increase of non-CARs which utilize sequential reactions for the solubility change, it is important to use as many reactive species as possible. If the resist sensitivity can be increased without the chemical amplification by making efficient use of active species generated by EUV/EB exposure, it will be a promising candidate for the resist having both high-sensitivity and low-LWR properties. In this study, a dual insolubilization resist used for EUV/EB lithography was proposed. The proposed resist was a negative-type polymer resist which utilizes polarity change and radical crosslinking, triggered by EUV/EB exposure. Polymers having triarylsulfonium cations and 2-hydroxy-2-methylpropiophenone as side chains were designed for realizing the dual insolubilization property. The cation moiety of 4-methacryloxyphenyldiphenylsulfonium methylsulfate (MAPDPS-MSA) or 4-methacryloxyphenyldibenzothiophenium methylsulfate (MAPBpS-MSA) was covalently bounded to the resist polymer (polymer-bounded onium cation, PBC) for the efficient use of thermalized electrons for the polarity change and the radical generation on the polymer structure. 2-[4-(2-hydroxy-2-methylpropionyl)phenoxy]ethylmethacrylate (IRG2959MA) was incorporated into the resist polymer as polymer-bounded radical generator (PBRG) unit to efficiently generate radicals on the polymer structures for the crosslinking. These two polymer radicals lead to crosslinking by the radical recombination, as illustrated in Fig.1-1.

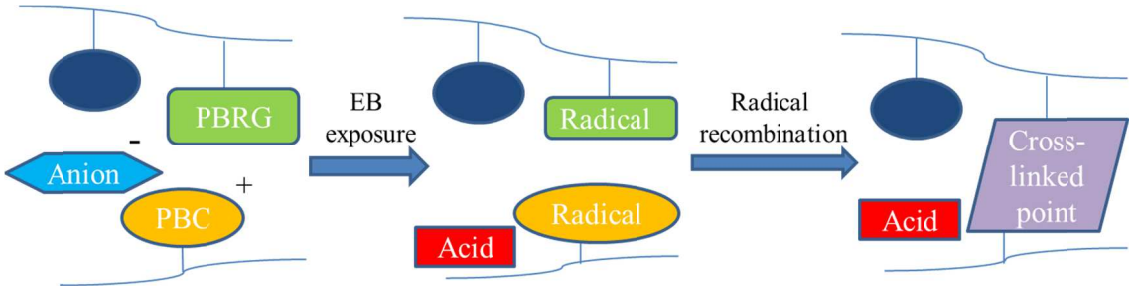

Fig.I-1 Concept of polymer radical generation and crosslinking.

1.2 Experimental Methods

1.2.1. Materials

MAPDPS-MSA and MAPBpS-MSA were synthesized in accordance with previous patent reports.[6,7] Phenylmethacrylate (PhMA), 3,3-dimethyl-3-hydroxypropanemethacrylate (HMBMA) and IRG2959MA were synthesized in accordance with a conventional esterification reaction. 3-methyladamantane-2-methacrylate (HAMA) was obtained from Osaka Organic Chemical Industry. The molecular structures of monomers are shown in Fig. I-2. Polymers were synthesized in accordance with the standard solution polymerization method using dimethyl-2,2'-azobis(2-methylpropionate) (V601) as an initiator. Five kinds of polymers were synthesized. After synthesis, the polymers were analyzed by ^{13}C-NMR for the determination of the composition ratio.

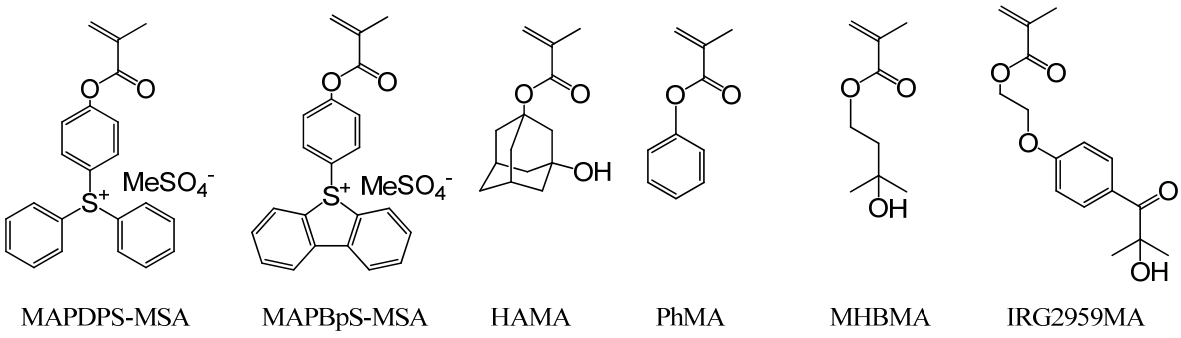

Fig. I-2 Molecular structures of monomers.

The viscosity of polymer solutions was measured to evaluate the difference of the molecular weights of synthesized polymers because the gel permeation chromatography is not suitable for the determination of the molecular weight of polymer electrolytes. 0.10 g of each polymer was dissolved in 0.6 ml solvent which was a mixture of cyclohexanone, ethyl lactate, and

γ-butylolactone with the volume ratio of 5:4:3. The viscosity [η] of each solution was measured at 25°C by a viscometer (Reologica Viscoanalyser VAR 100).

1.2.2. Sensitivity evaluation (E_0)

The proposed resists are a single component resist. The synthesized polymer was dissolved in the mixture of cyclohexanone, ethyl lactate, and γ-butylolactone with the volume ratio of 5:5:1 for a film forming. The weight ratio of polymer and solvent was 1:20. Hexamethyldisilazane (HMDS) was spin-coated at 2000 rpm for 20 sec on the surfaces of Si wafers and the coated wafers were baked at 110 °C for 60 sec. Then, the polymer solutions were spin-coated onto the surfaces of the Si wafers at 2000 rpm for 40 sec to form resist films. The prebake of the resist films was performed at 110 °C for 60 sec. The resist films with the thickness of 100 nm were obtained.

The mixture of acetonitrile and deionized water was used as a developer. The solubility of unexposed polymer increases with the acetonitrile concentration. The solution with the minimum concentration of acetonitrile for the complete dissolution of the unexposed polymer was selected as a developer for each polymer. The procedure to determine the minimum concentration of acetonitrile is as follows. The resist films were developed with the mixture of acetonitrile and deionized water for 60 sec at 25 °C and rinsed with deionized water for 30 sec. The concentration of acetonitrile was increased in steps of 2.5 volume % (vol %) until the resist film was completely dissolved in the solution within 60 sec.

The resist films were exposed to EUV radiations from EUV exposure system (Energetic EQ-10M). The exposure dose range was from 0.25 to 7.5 mJ/cm^2. After EUV exposure, the resist films were developed with the developer for 60 sec at 25 °C and rinsed with deionized water for 30 sec. The sensitivity (E_0) was defined by the exposure dose which gave 50 % film thickness, compared with the maximum film thickness after the sufficient exposure. The evaluated pattern was a 1 cm square pattern.

1.2.3 Acid generation efficiency evaluation

A coumarin 6 (C6) was used as an indicator to monitor the acid yield.[8)] A mixture of cyclohexanone, ethyl lactate, and γ-butylolactone, the volume ratio of which was 2:2:1, was used as a solvent. The weights of polymer components, solvent, and C6 were 300, 2000, and 8.8 mg, respectively. The resist solutions were spin-coated onto quartz substrates at 1000 rpm for 20 sec to form thin films. The prebake of the resist films was performed at 110 °C for 5 min. The resist films with approximately 0.6 μm thickness were obtained. The samples were exposed

to EUV radiations. The exposure dose range was from 3 to 12 mJ/cm^2. Then, the absorption spectra were recorded using an ultraviolet-visible (UV-VIS) spectrophotometer to measure acid yields on the basis of a characteristic absorption of the protonated form of C6.

1.2.4 Product analysis

The decomposition products upon exposure to EB were analyzed using high performance liquid chromatography (HPLC). The resist films of each polymer were prepared with the same procedure as that for the resist samples used for the sensitivity evaluation. The whole areas of resist films were exposed to 75 keV EB (Hamamatsu Photonics EB Engine) under N_2 atmosphere (oxygen density is less than 100 ppm). The exposure dose was 200 μC/cm^2. Then, the exposed polymers were removed from silicon substrates in 3.0 ml of 75 vol% acetonitrile aqueous solution. The acetonitrile solutions were directly analyzed by HPLC. The eluent was a solution of 80 vol% acetonitrile and 20 vol% water with 0.1 weight % (wt %) phosphoric acid. The flow rate of eluent was 0.5 ml/min. The column was Speriorex ODS 4.6×250 mm (Shiseido) with the temperature of 40 °C. The detector was a photodiode array (PDA) detector. The introduction volume was 20 μL (full volume of sample loop).

1.3 Results and discussion

1.3.1 Sensitivity

The composition ratios of synthesized polymers are listed in Table I-1. The viscosities of Polymers I-1-I-5 are listed in Table I-2. According to Mark-Howrink formula, the limiting viscosity [η] is expressed as where M, K, and α are viscosity-average molecular weight, and empirical parameters, respectively. K and α depend on the polymer-solvent interaction.

$$[\eta]=KM^{\alpha} \qquad (1\text{-}1)$$

Because of the similarity of the structures and composition ratio, K and α of the polymers used in this study are considered not to significantly differ from each other. In this study, the performance of solubility switching was evaluated using the sensitivity. However, the sensitivity of negative-type resists depends on the solubility of the unexposed polymer in the developer. A developer optimized for each polymer was used to avoid the effect of the molecular weight of unexposed polymer on the evaluation. Polymer I-5 was prepared to examine the validity of the evaluation method using the optimized developers. The solution with the minimum concentration of acetonitrile for the complete dissolution of the unexposed polymer was selected as a developer for each polymer, as described in the section 1.2.2. The minimum concentrations of acetonitrile for the complete dissolution of the unexposed polymers

are listed in Table I-3. The minimum exposure doses required for the solubility switching were evaluated using the developer optimized for each polymer.

Table I-1 Composition ratio of monomer units.

Sample	Composition ratio [mol%]					
	MAPDPS-MSA	MAPBpS-MSA	HAMA	PhMA	MHBMA	IRG2959 MA
Polymer I-1	29.3		22.3	21.4	27.0	
Polymer I-2	29.7		24.3	19.9		26.1
Polymer I-3		23.4	27.6	24.1	24.8	
Polymer I-4		27.4	29.0	18.9		24.7
Polymer I-5	26.4		28.0	19.3	26.4	

Table I-2 Viscosity of polymer solutions

Sample	Viscosity [mPa·s]
Polymer I-1	33.2
Polymer I-2	44.5
Polymer I-3	55.3
Polymer I-4	53.8
Polymer I-5	48.9

Table I-3 Acetonitrile concentration in developer, adjusted for each polymer.

Sample	Acetonitrile concentration [vol%]
Polymer I-1	17.5
Polymer I-2	20.0
Polymer I-3	25.0
Polymer I-4	30.0
Polymer I-5	25.0

The relationships between EUV exposure dose and the obtained normalized residual film thickness for Polymers I-1, I-2, I-3, I-4, and I-5 after rinsing are shown in Fig. I-3. The sensitivities (E_0s) were obtained to be 1.5, 0.9, 5.4, 0.7, and 1.3 mJ/cm^2 for Polymers I-1, I-2, I-3, I-4, and I-5, respectively. The viscosities of Polymers I-1 and I-5 were 33.2 and 48.9 mPa·s, respectively. The difference in E_0 caused by the viscosity was merely 0.2 mJ/cm^2. Therefore, the

molecular weight is not considered to significantly affect the evaluation of minimum exposure dose required for the solubility switching when the developer was optimized for each polymer.

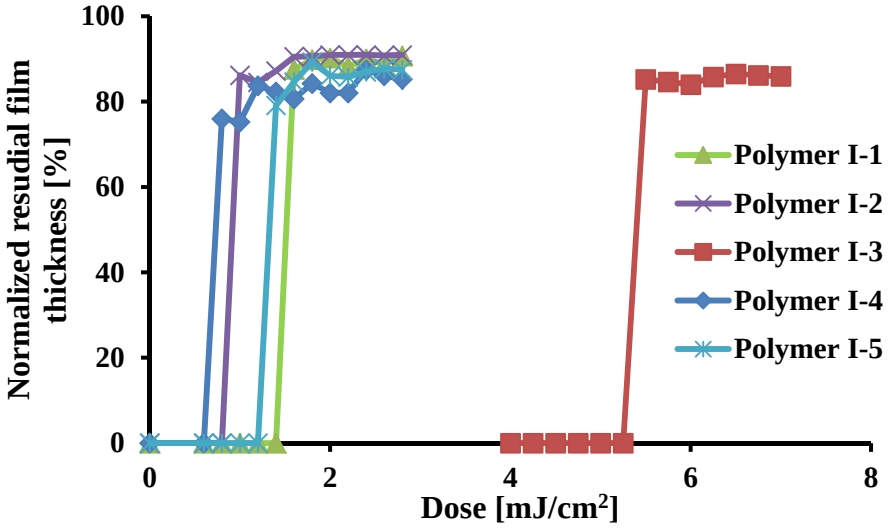

Fig. I-3 Sensitivity curves of Polymers I-1-I-5 upon exposure to EUV radiations.

The sensitivity of poly(methyl methacrylate) (PMMA) evaluated with the same apparatus was 25-85 mJ/cm^2.[9] The sensitivities of chemically amplified resists were 0.25-1.25 mJ/cm^2.[10] All polymers showed a highly sensitive negative-type response to EUV radiations, comparable to chemically amplified resists. Such a high sensitivity is considered to be attributed to the polarity change induced by the decomposition of PBC because even the polymers without a PBRG unit (Polymers I-1, I-3, and I-5) showed the highly sensitive property. For the effect of PBRG unit, the resist using Polymer I-2 that contained IRG2959MA showed about 1.7 times higher sensitivity (60% exposure dose) than the resist using Polymer I-1 that did not contain IRG2959MA. Similarly, the resist using Polymer I-4 that contained IRG2959MA showed about 7.7 times higher sensitivity (13% exposure dose) than the resist using Polymer I-3 that did not contain IRG2959MA. The PBRG unit is also considered to have contributed to the sensitivity enhancement. IRG2959MA is a well-known compound to generate radicals through Norrish type 1 reaction via its triplet excited state upon exposure to UV light (Fig.I-4).[11-13] Upon exposure to EUV radiations, the triplet excited state of IRG2959MA is generated through the internal conversion following the direct electronic excitation by a secondary electron or the charge recombination between a IRG2959MA radical cation and a thermalized electron. Generally, the ratio of the electronic excited states of solutes generated through the direct excitation by secondary electrons is low unless the solute concentration is significantly high.

The ratio of electronic excited states generated through the charge recombination is also low in the presence of the electron scavenger such as onium salts. Nevertheless, the incorporation of IRG2959MA increased the sensitivity as shown in Fig. I-3. This result suggests that the concept of the use of radical crosslinking works well. The contribution of the radical cations of monomer units to crosslinking is later discussed.

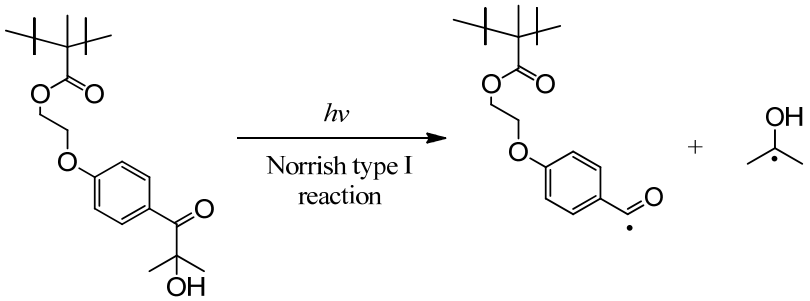

IRG2959MA

Fig.I-4 Radical generation process of IRG2959MA thorough Norrish type 1 reaction.

MAPDPS-MSA and MAPBpS-MSA, the two aromatic rings of which were covalently connected, were utilized for PBC, as shown in Fig. I-2. These units are decomposed by the reaction with the thermalized electrons (dissociative electron attachment).[2)] Their reaction schemes through dissociative electron attachment are shown in Fig. I-5. The polarity of PBC units changes from polar to non-polar by the decomposition of PBC. The reduction potentials of triphenylsulfonium (TPS) cation and phenyl dibenzothiophenium (PBpS) are -1.35 and -0.67 V, respectively.[14)] MAPBpS-MSA is considered to have a lower reduction potential than MAPDPS-MSA. It has been reported that the lower the reduction potential, the higher the efficiency of dissociative electron attachment.[15)] Therefore, it was expected that the sensitivities of Polymers I-3 and I-4 with MAPBpS-MSA should be higher than those of Polymers I-1, I-2, and I-5 with MAPDPS-MSA. However, the results were inconclusive, as shown in Fig. I-3. The effect of these onium salts on the polarity change does not seem to differ. The measurement of acid generation efficiency and the analysis of decomposed products were carried out to clarify the reaction mechanism.

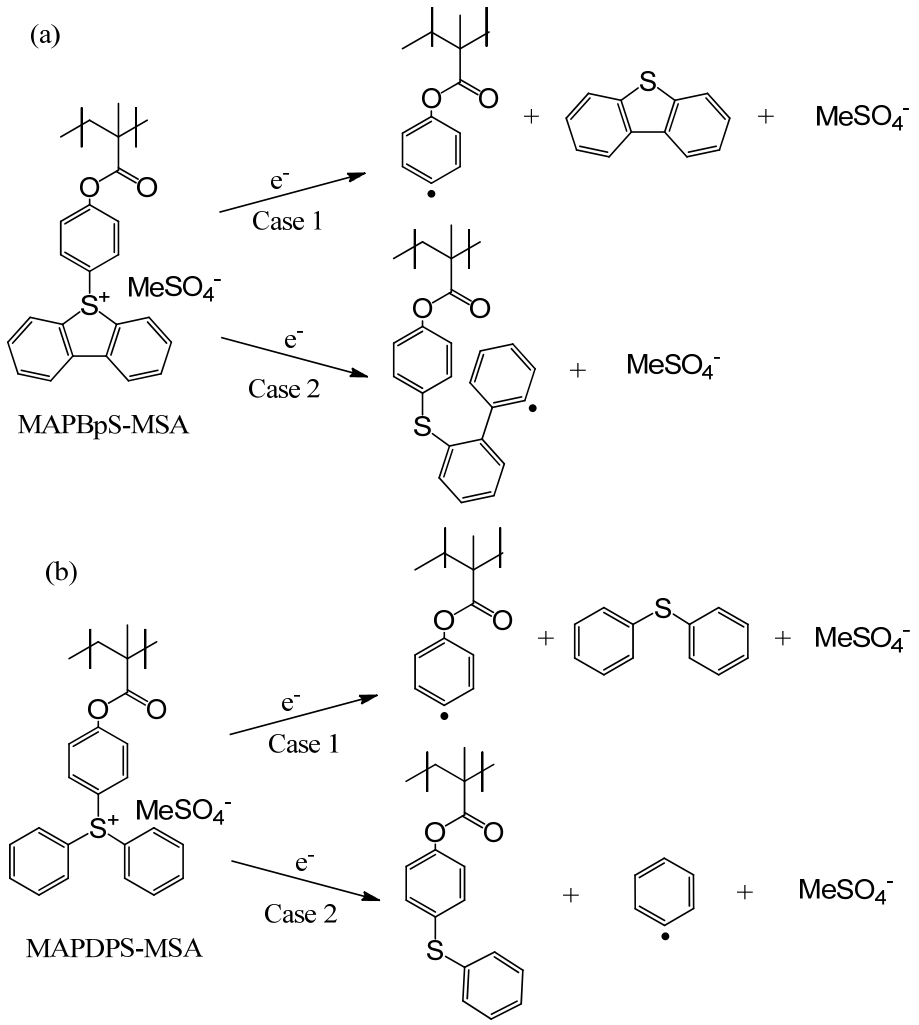

Fig I-5 Reduction processes of MAPBpS and MAPDPS cations through dissociative electron attachment.

1.3.2 Acid generation efficiency

The acid yields of Polymers I-1-I-5 were determined by the UV-VIS spectrophotometric titration of protonated C6 absorption. After exposure to EUV radiations, an absorption band appeared at 533 nm. This indicated that C6 switched to protonated C6. The absorption intensity was plotted against the exposure dose in Fig. I-6. The acid generation efficiencies were evaluated from the slopes of the graphs in Fig I-6. Table I-4 shows the relative acid generation efficiency, normalized with that of Polymer I-1. The relative acid generation efficiencies of the polymers with MAPBpS-MSA were significantly lower than those of polymers with MAPDPS-MSA despite our expectation, even if the difference of composition ratio (Table I-1) was taken into account. Table I-5 shows the quantum efficiencies of acids generated through the direct electronic excitation with 254 nm wavelength photons.[14] The quantum efficiency of PBpS is 41 % that of TPS. The composition ratio of the PBC units of Polymers I-1-I-5 is 23-30

mol%, which corresponds to roughly 40-50 wt%. Therefore, the acid generation through the electronic excitation by secondary electrons is not negligible. The results shown in Table I-4 are likely to strongly reflect the effect of the electronic excitation by secondary electrons. The presumed reaction schemes of acid generation through the electronic excited states are shown in Fig. I-7.

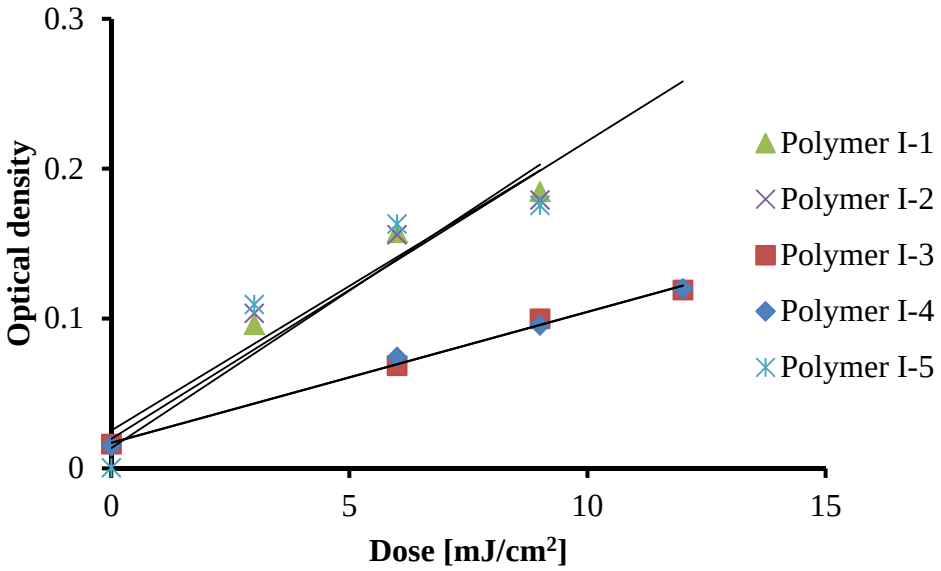

Fig. I-6 Dependence of optical density of protonated Coumarin6 on EUV exposure dose

Table I-4 Relative acid generation efficiency, normalized by the acid generation efficiency in Polymer I-1.

Sample	Relative acid generation efficiency*
Polymer I-1	1.00
Polymer I-2	0.95
Polymer I-3	0.41
Polymer I-4	0.41
Polymer I-5	0.92

*Normalized by the acid generation efficiency in Polymer I-1.

TableI-5 Quantum yield of acids for TPS and PBpS upon exposure to light with the wavelength of 254 nm.[14]

Triarylsulfonium salt	Quantum yield (254nm)
TPS	0.66
PBpS	0.27

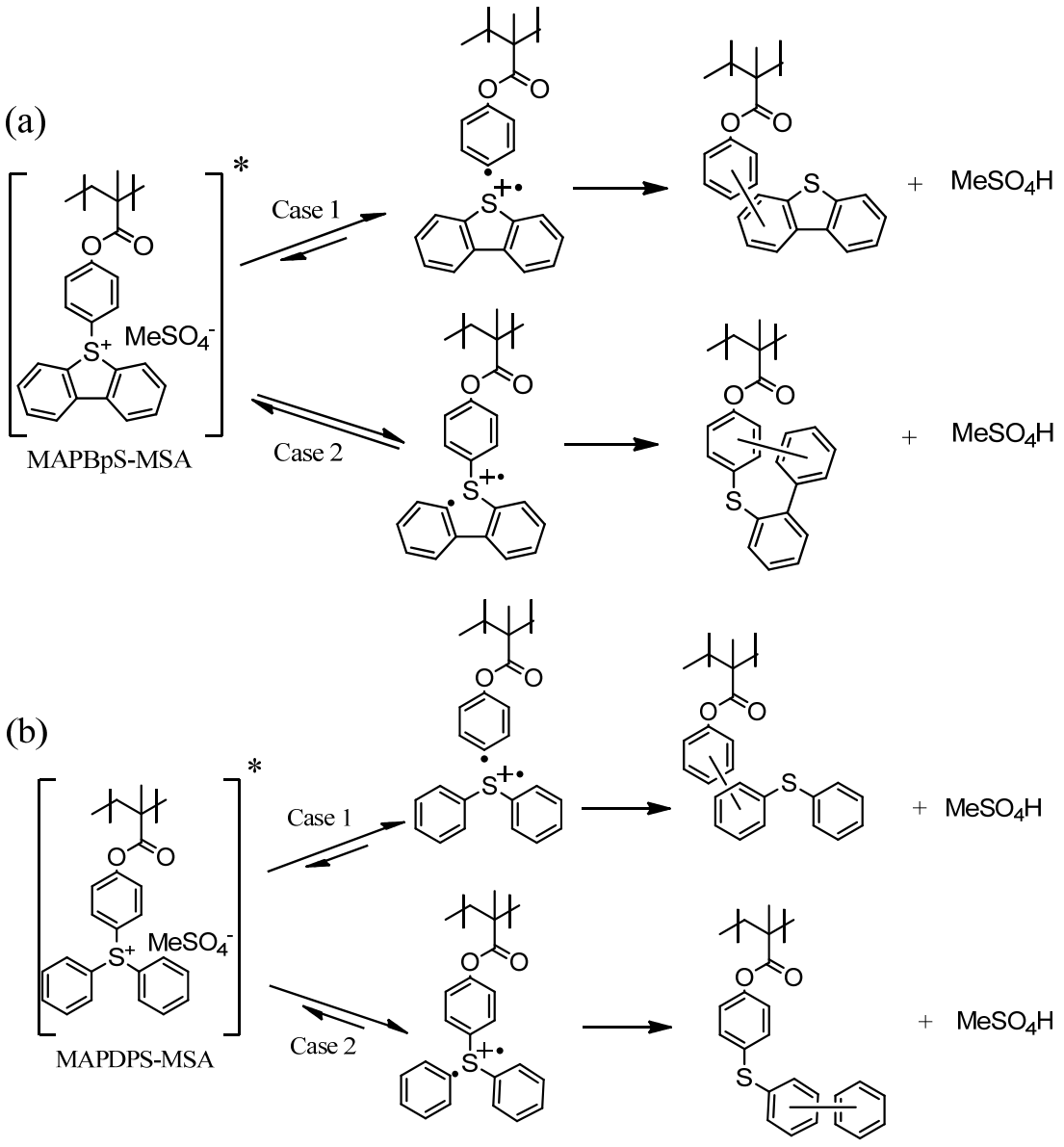

Fig. I-7 Acid generation processes of MAPBpS and MAPDPS cations through electronic excitation state without external proton sources.

In the acid generation though the dissociative electron attachment, the polymers play an important role. The protons of acids are generated through the deprotonation of polymer radical cations.[16] As shown in Fig. I-6, the acid yield did not depend on the MHBMA / IRG2959MA units. This result indicates that the deprotonation efficiency of IRG2959MA radical cation is approximately the same as that of MHBMA radical cation, if their radical cations are deprotonated. Upon exposure to EUV radiations, HAMA and PhMA units are also ionized and their radical cations are generated. These radical cations are also a possible proton source. In other words, neutral radicals are generated after the deprotonation of radical cations. Although the deprotonation efficiency of the radical cations of each unit is unknown, Fig. I-6 suggests that the amount of neutral radicals generated through the radical cations of Polymer I-1 are the same as that generated through the radical cations of Polymers I-2 and I-5. Similarly, the amounts of neutral radicals generated through the radical cations of Polymer I-3 are probably the same as that generated through the radical cations of Polymer I-4. These neutral radicals are considered to contribute to the crosslinking of polymers, in addition to the radicals generated through the triplet excited states of IRG2959MA discussed in the section 1.3.1.

1.3.3 Product analysis

Polymers I-1 and I-3 were analyzed by HPLC after the exposure to EB. The HPLC chromatograms of Polymers I-1 and I-3 are shown in Fig. I-8. Diphenyl sulfide (DPS) and biphenyl were detected as the decomposed products of Polymer I-1 (Chart A). The biphenyl is considered to be generated by the radical recombination between phenyl radicals. Dibenzothiophene (BpS) was detected as the decomposed product of Polymer I-3 (Chart B). These results strongly supported the reaction scheme shown in Fig. I-5. As indicated by the absorption intensities (areas) of DPS and BpS (Table I-7), BpS yield was estimated two and half times larger than DPS yield. The ratio between Cases 1 and 2 in Fig. I-5 (b) is probably 1:2 because the scission probabilities of three C-S bonds are not considered to differ from each other. In that case, the biphenyl yield should be the same as DPS yield. However, the biphenyl yield was 36 mol% DPS yield. This is because the phenyl radicals were quenched by oxygen in the ambient air during the delay time between the exposure and HPLC analysis. The radical recombination of phenyl radicals with other radicals is also considered to be the reason for the low yield of biphenyl radicals. Although the ratio between Cases 1 and 2 in Fig. I-5(a) is unknown, the amount of radicals remaining on Polymer I-3 for PBC units was at least two and half times more than that remaining on Polymer I-1 for PBC units, considering the difference between BpS and DPS yields. However, the effect of polarity change, which is mainly

determined by the total decomposition yield of PBC units, is higher in Polymer I-1 than in Polymer I-3, as indicated by their acid generation efficiencies (Fig. I-6). The reason why the effects of MAPBpS-MSA and MAPDPS-MSA on the polarity change did not seem to differ is considered to be that the difference between the effects of PBC units on polarity change and radical generation for crosslinking was balanced out.

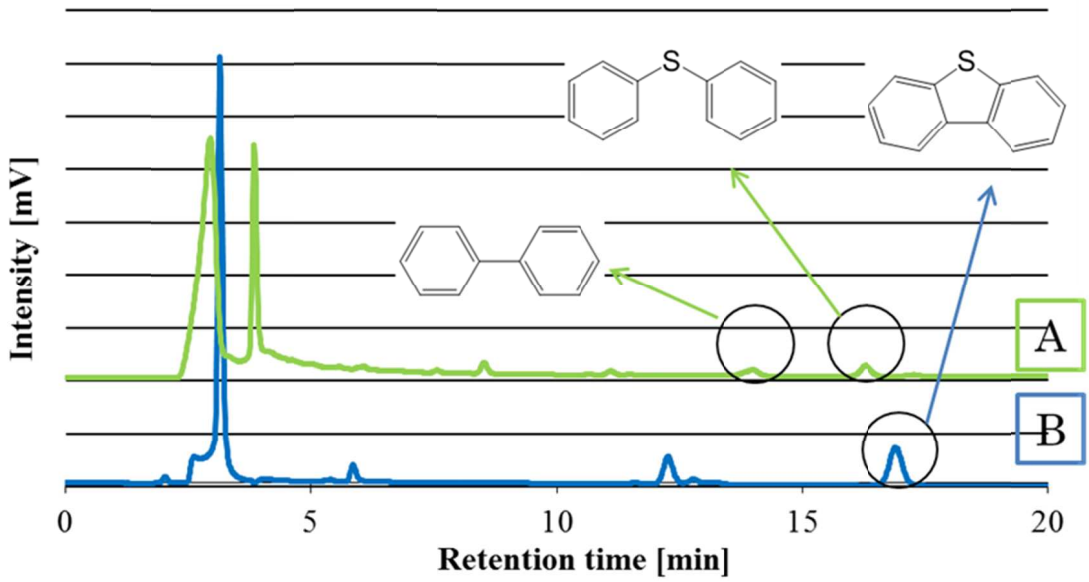

Figure I-8 HPLC chromatogram of EB irradiated films. Chart A: Polymer I-1 (greenish yellow line) Chart B: Polymer I-3 (Blue line).

Table I-6 Yields of decomposition products of Polymers I-1 and I-3.

Product	Peak area [Abs. 254nm]	Molar absorptivity at 254nm [l/mol・cm]
Diphenyl sulfide	172391	2260
Biphenyl	101058	3714
Dibenzothiophene	643239	3333

1.4 Conclusion

The dual insolubilization resists used for EUV and EB lithography were proposed. The proposed resists were a negative-type polymer resist which utilizes polarity change and radical crosslinking triggered by EUV/EB exposure. Polymers having triarylsulfonium cations and 2-hydroxy-2-methylpropiophenone as side chains were designed for realizing the dual insolubilization property. 2-hydroxy-2-methylpropiophenone was incorporated to efficiently generate radicals on the polymer structures for crosslinking. The effect of

2-hydroxy-2-methylpropiophenone was confirmed. Onium salt was incorporated for the efficient use of thermalized electrons for the polarity change and radical generation. For the effects of onium salts, MAPBpS-MSA and MAPDPS-MSA were compared. MAPBpS-MSA was superior to MAPDPS-MSA for the radical generation on the polymer structure. MAPDPS-MSA was superior to MAPBpS-MSA for the polarity change. The designed polymer showed highly sensitive property.

1.5 References

1) T. Kozawa, J. J. Santillan, and T. Itani, Jpn. J. Appl. Phys. **52**, 076502 (2013).

2) K. Natsuda, T. Kozawa, and K. Okamoto, A. et al. Jpn. J. Appl. Phys. **48**, 06FC05 (2009).

3) V. Canalejas, J. Mater. Chem. C **1**, 1392 (2013).

4) A. E. Grigorescu and C. W. Hagen, Nanotechnology **20**, 292001 (2009).

5) V. Singh, V. S. V. Satynarayana, S. K. Sharma, and S. Ghosh, et al. Proc. SPIE **9051**, 905106 (2014).

6) K. Ichikawa and T. Masuyama, JP5746836 (2015).

7) J. Iwabuchi and Y. Osawa, US2007/219368 (2007).

8) H. Yamamoto, T. Kozawa, and A. Nakano, et al. Jpn. J. Appl. Phys. **43**, L848 (2004).

9) A. Konda, H. Yamamoto, and S. Yoshitake, et al. Proc. SPIE **9776**, 977629 (2016).

10) H. Kudo, S. Matsubara, and H. Yamamoto et al. J. Polym. Sci., Part A: Polym. Chem. **53**, 2343 (2015).

11) M. Liu, M.-D. Li, and J. Xue, et al. J. Phys. Chem. A **118**, 8701 (2014).

12) K. Vacek, J. Geimer, and D. Beckert, et al. J. Chem. Soc., Perkin Trans. **2**, 2469 (1999).

13) N. S. Allen, M. C. Marin, and M. Edge, et al. J. Photochem. Photobiol. A: Chem. **126**, 135 (1999).

14) C. Selvaraju, A. Sivakumar, and P. Ramamurthy, J. Photochem. Photobiol. A: Chem. **138**, 213 (2001).

15) S. Tarutani, H. Tsubaki, and H. Takahashi, et al. Proc. SPIE **7639**, 763909 (2010).

16) A. Nakano, T. Kozawa, and K. Okamoto, et al. Jpn. J. Appl. Phys. **45**, 6866 (2006).

Chapter II

Effects of organotin compound on radiation-induced reactions of extreme-ultraviolet resist utilizing polarity change and radical crosslinking

2.1. Introduction

To reduce pattern defects due to the stochastic effect at a half-pitch of less than 15 nm, some ideas for improving the sensitivity of CARs have been studied to reduce the acid diffusion length of chemical reactions.[1-3] A multi-trigger resist[4], anisotropic acid diffusion[5-7] are among them. However, stochastic effect due to luck of EUV absorption cross section still have remained by using conventional organic resists. Thereby, metal resist platforms have attracted much attention as a mean of increasing the EUV photon absorption efficiency. These resists have been avidly investigated and reported as being comparable to CARs in the lithography performances.[8-10] However, some of these resist solutions lack long-term storage stability expected to be aggregated the metal component,[11] and their mechanisms of solubility change are still poorly understood. Understanding the sensitization and reaction mechanisms of high-EUV-absorption materials is important to control the patterning image and sensitivity of resists. In particular, the elucidation of the effects of organic metal compounds on the sensitization and reaction mechanisms of CARs is expected to provide the valuable information for overcoming the RLS trade-off. Although the organic metal compounds have a larger EUV absorption cross section than organic compounds, the ionization energies of organic metal compounds are similar to those of organic compounds. The comparison between metal organic compounds and organic compounds formulated into the same resist platform is helpful to understand the metal-induced effects on the resist chemistry.

In this study, an organotin compound was incorporated in the polymer chain to increase the EUV absorption of the dual insolubilization resist. The organotin compound used was triphenyl(4-vinylphenyl)stannane (TPSnSt). The effect of the organotin compound on the sensitivity was investigated from the viewpoint of radiation-induced reactions. Although the dual insolubilization resist is a non-CAR, knowledge about the radiation-induced reactions of organotin compounds is expected to be useful for the design of CARs.

2.2 Experimental methods

2.2.1 Materials

MAPDPS-MSA and MAPBpS-MSA were prepared as described in section 1.2.1., TPSnSt was synthesized in accordance with the previous report.[12] 4-tritylphenylmethacrylate (TPMMA) was synthesized by a conventional esterification reaction. Polymers were synthesized and analyzed by same procedure described in section 1.2.1.The details of polymer properties are shown in Table II-1. The molecular structures of monomers are shown in Fig. II-1.

Molecular weights were determined by performing gel permeation chromatography (GPC) analysis with an OHpak 806M HQ column (Shodex) using a Shodex GPC-101 system. 100 mM LiBr *N*,*N*-dimethylformamide (DMF) solution was used as an eluent at a flow rate of 1.0 mL/min and a column temperature of 70 °C. The detector was a UV detector and the monitored wavelength was 270 nm. The introduction volume was 100 μL (full volume of sample loop). The molecular weights determined using polystyrene standards are also listed in Table II-1. The GPC analysis is not accurate enough for the comparison of the molecular weight of polymers containing different electrolytes (MAPBpS-MSA and MAPDPS-MSA) because the efficiency of adhesion to the base material of column depends on the polarity of the electrolyte. The molecular weights of Polymers II-1 and II-3 were considered to be more underestimated than those of Polymers II-2 and II-4, because the adhesion efficiencies of Polymers II-1 and II-3 were slightly higher than those of Polymers II-2 and II-4 owing to the higher polarity of MAPDPS-MSA.

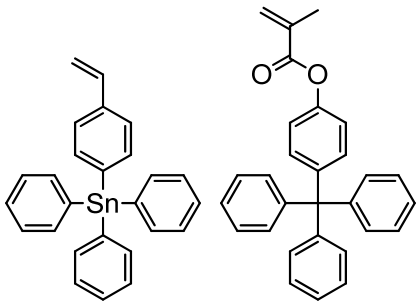

TPSnSt TPMMA

Fig. II-1. Molecular structures of monomers.

Table II-1 Composition ratio of monomer units and polymer properties.

Sample	Composition ratio (mol%)					Molecular weight (Mw)	Dispersity (Mw/Mn)
	MAPDPS-MSA	MAPBpS-MSA	TPSnSt	TPMMA	IRG2959MA		
Polymer II-1	24.1		55.5		20.4	35500	13.7
Polymer II-2		24.1	55.5		20.4	73200	6.6
Polymer II-3	24.4			57.3	18.4	19200	12.7
Polymer II-4		24.2		57.0	18.8	32500	4.1

2.2.2 Film density evaluation

The polymer (resist) solutions used for the film density evaluation were prepared by dissolving 0.10 g of each polymer in 2.0 ml solvent, which was a mixture of cyclohexanone, ethyl lactate, and γ-butyrolactone with a volume ratio of 5:4:1. The resists used were single component resists. The polymer solutions were spin-coated at 3000 rpm for 40 s and baked at 110 °C for 60 s to obtain thin films with approximately 50 nm film thickness. The polymer films were analyzed by an X-ray diffractometer (Rigaku Smart Lab.). The linear attenuation coefficients of the films for EUV (92.5 eV) were calculated from the film density and photon absorption cross section data.[13] The photon absorption cross sections for 92.5 eV were calculated by a linear approximation method using date for 91.5 and 108.5 eV given in Ref. 13. The stopping powers and continuous slowing down approximation (CSDA) ranges of 75 keV electrons were calculated by the ESTAR program provided by National Institute of Standards and Technology (NIST).

2.2.3 Sensitivity (E_0) evaluation

The sensitivity evaluation samples and developers for each polymer were prepared by the same procedure as described in Section 1.2.2. Selected developers as the developer for each polymer were shown in Table II-2. Since Polymer II-4 did not dissolve in the mixture of acetonitrile and water, as shown in Table II-2, a mixture of acetonitrile, methyl ethyl ketone (MEK), and water was applied to the development of Polymer II-4. The volume ratio of acetonitrile, MEK, and water was 25.0:25.0:50.0.

The polymer films were exposed to EUV radiation by the same procedure described in section 1.2.2. The exposure dose range was applied from 0.25 to 3.0 mJ/cm^2 in this experiment.

Table II-2 Acetonitrile concentration in developer, optimized for each polymer.

Sample	Acetonitrile concentration [vol%]
Polymer II-1	37.5
Polymer II-2	45.0
Polymer II-3	50.0
Polymer II-4	Not developable

2.2.4 Acid generation efficiency evaluation

2.2.4.1 EUV

The evaluation samples for acid generation efficiency were prepared by the same procedure as described in Section 1.2.3. The film thicknesses were 471, 389, 463, and 408 nm for Polymers II-1-II-4, respectively. The samples were exposed to EUV radiation. The exposure dose range was from 3 to 9 mJ/cm^2. Then, the acid yields were measured the same procedure as described section 1.2.2.

2.2.4.2 75 keV EB

The polymer films used for the evaluation of acid yields generated upon exposure to a 75 keV EB were prepared by the procedure described in the section 2.2.4.1. The film thicknesses were 517, 600, 481, and 435 nm for Polymers II-1-II-4, respectively. The polymer films were irradiated by a 75 keV EB with an exposure dose from 20 to 80 $\mu C/cm^2$ using an EB exposure system (Hamamatsu Photonics EB Engine).

2.2.5 Product analysis

The polymers (Polymer II-5 and II-6) were synthesized by the same standard solution polymerization method as Polymers II-1-II-4 and the composition ratio was determined by ^{13}C-NMR (Table II-3). The polymer solutions used for the product analysis were prepared by dissolving 0.10 g of each polymer in 1.0 ml cyclohexanone. Prepared samples were slit-coated to obtain wet films with 61 μm thickness, using a Barcoater (Rod No. 24 YASUDA SEIKI). The film thickness after prebaking at 110 °C for 5 min. was adjusted to be approximately 2.0 μm. After the coating, the whole area of the samples was exposed to a 75 keV EB under a N_2 atmosphere (oxygen density was less than 100 ppm). The exposure dose range was 20-100 $\mu C/cm^2$. Then, each exposed polymer film was removed from its silicon substrate in 2.0 ml of tetrahydrofuran (THF). The THF solutions were directly analyzed by GPC with directly connected TSKgel $G2000H_{XL}$, $G3000H_{XL}$, $G4000H_{XL}$, and $G5000H_{XL}$ columns using a Shodex GPC-101 system. THF was used as an eluent at a flow rate of 0.6 mL/min and a column temperature of 40 °C. The molecular weights of the polymers were determined using polystyrene standards. The detector was a refractometer. The volume of introduced polymer solution was 100 μL (full volume of sample loop).

Table II-3 Composition ratio of monomer units and polymer properties.

Sample	Composition ratio (mol%)			Molecular weight (Mw)	Dispersity (Mw/Mn)
	TPSnSt	TPMMA	IRG2959MA		
Polymer II-5	82.4		17.6	7400	1.8
Polymer II-6		80.6	19.4	9300	2.0

2.3. Results and discussion

2.3.1 Film density evaluation

The film densities of tin-containing polymers (Polymers II-1 and II-2) were evaluated for the calculation of linear attenuation coefficients of resist films. TPSnSt was replaced with TPMMA (Polymers II-3 and II-4), which does not contain tin, to investigate the effects of tin on the linear attenuation coefficients. The measured film densities and calculated linear attenuation coefficients are listed in Table II-4. The film densities of the tin-containing polymers were approximately 1.1 times higher than those without tin (Sn) owing to the heavy weight of tin atoms. Tin is well known to have a larger EUV photon absorption cross section than the typical elements used in EUV resists, as shown in Table II-5. However, the linear attenuation coefficients of TPSnSt-containing polymers were only 1.3 times higher than those of the TPMMA-containing polymers despite a tin composition of at least 15 wt%. This is because the oxygen ratios were decreased from 14.3 to 9.7 wt% with the increase of tin ratios by replacing TPMMA with TPSnSt, as shown in Table II-6. The carbon ratio should be reduced in the future design of high-absorption resists because the low photon absorption cross section of carbon is the essential reason for the low EUV absorption of resists.

The stopping powers and CSDA ranges of all the polymers for 75 keV electrons were approximately the same, as shown in Table II-4. Note that the inverse of the CSDA range is roughly equivalent to the linear attenuation coefficient. Since an electron is a charged particle, the beam intensity is decreased through the interaction with the electrons of constituent atoms. Therefore, the CSDA range is approximately determined by the density of electrons. The reason why there was little difference among the 75 keV CSDA ranges is that the densities of the polymers are approximately the same.

Table II-4. Film densities, linear attenuation coefficients, stopping powers, and CSDA ranges.

Sample	Film density [g/cm^3]	μ [/μm] 92.5 eV EUV	Stopping power [eV/nm] 75 keV EB	CSDA range [μm] 75 keV EB
Polymer II-1	1.34	5.64	0.597	73.5
Polymer II-2	1.32	5.55	0.586	74.8
Polymer II-3	1.21	4.19	0.575	76.1
Polymer II-4	1.25	4.33	0.593	73.7

Table II-5 Photon absorption cross section of elements at 92.5 eV.

	Photon absorption cross section [cm^2/g]				
	C	H	O	S	Sn
92.5 eV*	2.89×10^4	1.48×10^4	7.84×10^4	1.60×10^4	9.11×10^4

*Obtained by interpolation of the data in Ref. 13.

Table II-6 Elemental ratio of polymers.

	Elemental ratio [wt%]				
	C	H	O	S	Sn
Polymer II-1	66.2	5.2	9.3	3.6	15.7
Polymer II-2	66.3	5.0	9.3	3.7	15.7
PolymerII-3	76.0	5.8	14.3	3.9	0
Polymer II-4	76.1	5.7	14.3	3.9	0

2.3.2 Sensitivity evaluation

The sensitivities of Polymers II-1 to II-4 were evaluated to investigate the effect of tin on the sensitivity. Fig. II-2 shows the relationship between the EUV exposure dose and the normalized residual film thickness after rinsing for Polymers II-1 to II-4. Note that the necessity and validity of optimizing the developer for each polymer used for the sensitivity evaluation have been mentioned in chapter 1. The sensitivities (E_0s) were evaluated to be 0.6, 0.6, 1.5, and >3.0 mJ/cm^2 for Polymers II-1, II-2, II-3, and II-4, respectively. The sensitivities of the TPSnSt-containing polymers were higher than that of Polymer II-3, which did not contain TPSnSt. Polymer II-4 did not become insoluble at exposure doses of less than 3 mJ/cm^2. As mentioned in the section 2.2.3, MEK was added to the developer for Polymer II-4 because it did not dissolve in the mixture of acetonitrile and water, unlike the other polymers. The dielectric constants of MEK and acetonitrile are 18.6 and 30.5, respectively. An appropriate solvent with

higher dielectric constant than that of MEK is necessary to obtain sufficient contrast with the low exposure dose for Polymer II-4. Comparing Polymers II-1 and II-2, MAPDPS-MSA is more suitable than MAPBpS-MSA because a highly polar developer can be used even when it is copolymerized with a low polarity unit such as TPMMA. This feature is advantages for the material design because the range of monomer units that can be incorporated becomes large.

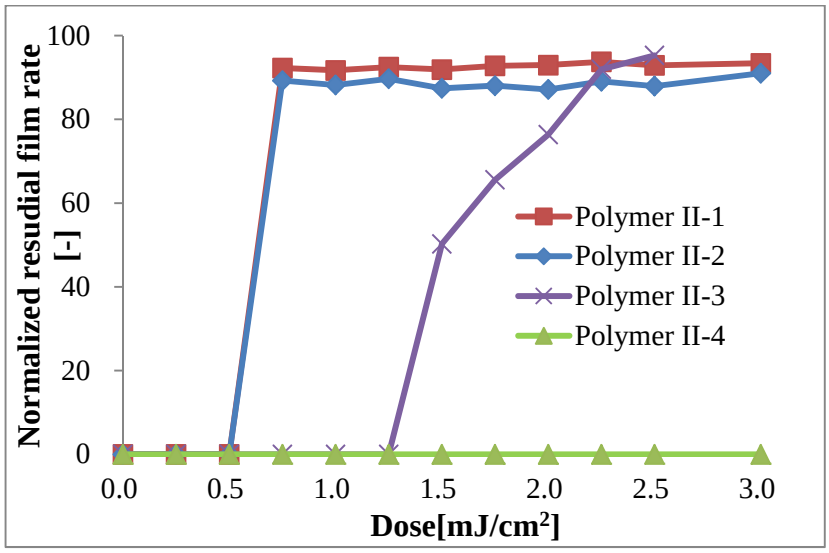

Fig. II-2. Sensitivity curves of Polymers II-1-II-4 upon exposure to EUV radiation.

The sensitivities of Polymers II-1 and II-2 were the same upon exposure to EUV. MAPBpS-MSA, which has a lower reduction potential than MAPDPS-MSA, is considered to show a higher decomposition efficiency than MAPDPS-MSA by the dissociative electron attachment of thermalized electrons.[13] Therefore, Polymer II-2 was expected to be more sensitive than Polymer II-1. The polymers examined utilize the polarity change and radical crosslinking to change the solubility (insolubilization) of polymers in the developer. The radiation-induced reactions of MAPDPS-MSA and MAPBpS-MSA were investigated using the polymers without TPSnSt as descrided in chapter 1. The contribution of MAPDPS-MSA to the two insolubilization reactions was different from that of MAPBpS-MSA. MAPBpS-MSA was superior to MAPDPS-MSA in terms of radical generation on the polymer structure, whereas MAPDPS-MSA was superior to MAPBpS-MSA in terms of the polarity change. Similarly to in the case of chapter 1, the reason why the effects of MAPBpS-MSA and MAPDPS-MSA on the sensitivity did not differ seems to be that the difference between the effects of PBC units on the polarity change and radical generation to induce crosslinking canceled each other out. The effects of TPSnSt on the reaction mechanisms of dual insolubilization resist is discussed on the basis of the evaluation of acid generation efficiency and the product analysis in later sections.

2.3.3 Acid generation efficiencies

The acid yields of Polymers II-1-II-4 were determined by the UV-VIS spectrophotometric titration of protonated C6 absorption to investigate the decomposition of PBC units. In particular, the interaction of TPSnSt with the decomposition process of PBC units is discussed. After exposure to EUV or 75 keV EB radiation, an absorption band appeared at 533 nm. This indicated that C6 switched to protonated C6. The absorption intensity was plotted against the exposure dose in Figs. II-3 and II-4. The absorption intensity was normalized with the film thickness. The acid generation efficiencies were evaluated from the slopes of the graphs in Fig. II-3 and II-4 by taking into account the differences in the film thickness and linear attenuation coefficient. Table II-7 shows the relative acid generation efficiency for EUV irradiation. The acid generation efficiencies were normalized with that of Polymer II-1. Table II-8 shows the relative acid generation efficiency upon EB irradiation, normalized with that of Polymer II-1 by taking into account the stopping power. Except for Polymer II-1 upon exposure to EUV, the acid generation efficiency was increased by approximately 10% by the addition of TPSnSt (comparisons between Polymers II-2 and II-4 for EUV and EB and comparison between Polymers II-1 and II-3 for EB). Although the positive effect of TPSnSt on the acid generation efficiency is still inconclusive, there was no negative effect. This means that TPSnSt interferes with neither the reaction of the PBC unit with thermalized electrons nor the proton generation reaction. In the enhancement of resist absorption using fluorine, the fluorination of polymers even interferes with the proton generation reaction in a particular case.[14] Aryl or alkyl stannic compounds are known to react readily with strong acids such as hydrochloric acid and triflic acid below room temperature to generate a stannic chloride and a stannic trifluoromethanesulfonate, resepectively. [15,16] Although the TPSnSt concentration was approximately 15.7 times higher than the C6 concentration, TPSnSt did not affected the evaluation of acid generation efficiency.

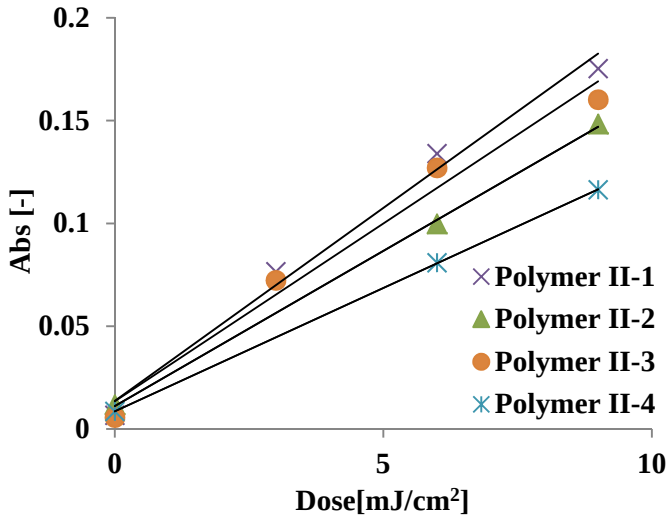

Fig. II-3. Dependence of optical density of protonated C6 on EUV exposure dose.

Table II-7 Relative acid generation efficiency upon exposure to EUV radiation.

Sample	Relative acid generation efficiency*
Polymer II-1	1.00
Polymer II-2	0.69
Polymer II-3	0.98
Polymer II-4	0.62

*Normalized with the acid generation efficiency of Polymer II-1, by taking into account the differences in the film thickness and linear attenuation coefficient.

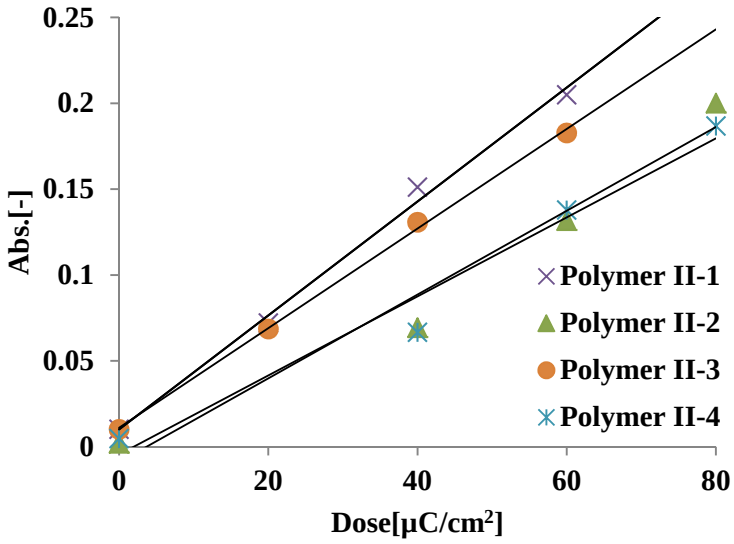

Fig. II-4 Dependence of optical density of protonated C6 on EB exposure dose.

Table II-8 Relative acid generation efficiency upon exposure to EB

Sample	Relative acid generation efficiency*
Polymer II-1	1.00
Polymer II-2	0.75
Polymer II-3	0.90
Polymer II-4	0.69

*Normalized with the acid generation efficiency of Polymer II-1, by taking into account the difference in the stopping power.

The relative acid generation efficiencies of the polymers with MAPBpS-MSA were approximately 20-30 % lower than those of the polymers with MAPDPS-MSA, as shown in Tables II-7 and II-8. In the acid generation result of chapter 1, the acid generation efficiencies of the polymers with MAPBpS-MSA were approximately 40 % of those of the polymers with MAPDPS-MSA (60% reduction). Although the composition ratios of the PBC units of the polymers used in the studies of chapter 1 was 23-30 mol%, similarly to in this study, these composition ratios correspond to roughly 40-50 wt % concentration. The concentration of PBC units in this study corresponds to roughly 30 wt%, which is significantly lower than that in the result of chapter 1. The acids were mainly generated through a reduction process by the dissociative electron attachment of thermalized electrons in the polymers with MAPBpS-MSA, while the acids generated through the electronic excitation significantly contributed to the total acid yield for the polymers with MAPDPS-MSA as descrided in chapter 1 because of the high concentration of 40-50 wt%. Because of the low concentration of PBC units, the contribution of acids generated through the electronic excitation was considered to be smaller in this study. Consequently, the difference in the acid generation efficiencies of the polymers with MAPDPS-MSA and MAPBpS-MSA decreased from 60 to 20-30 %.

As discussed above, TPSnSt was not considered to affect the decomposition of triarylsulfonium cations. However, the sensitivity of Polymer II-1 was more than 2.5 times higher than that of Polymer II-3. Such enhancement exceeds the value expected from the difference in the EUV linear attenuation coefficient. It is known that excited aryl or alkyl stannic compounds generate two radicals through Sn-C bond scission from the triplet excitation state, as shown in Fig. II-5.[17] The generated Sn radicals connected to the polymer chain may

lead to crosslinking by the radical recombination with the other polymer radicals, as shown in Fig. II-6. The effect of TPSnSt on crosslinking is discussed in the next section.

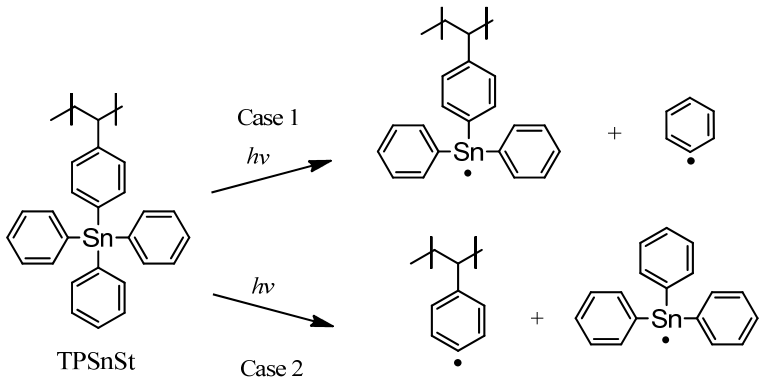

Fig. II-5 Radical generation processes of TPSnSt through photodecomposition.

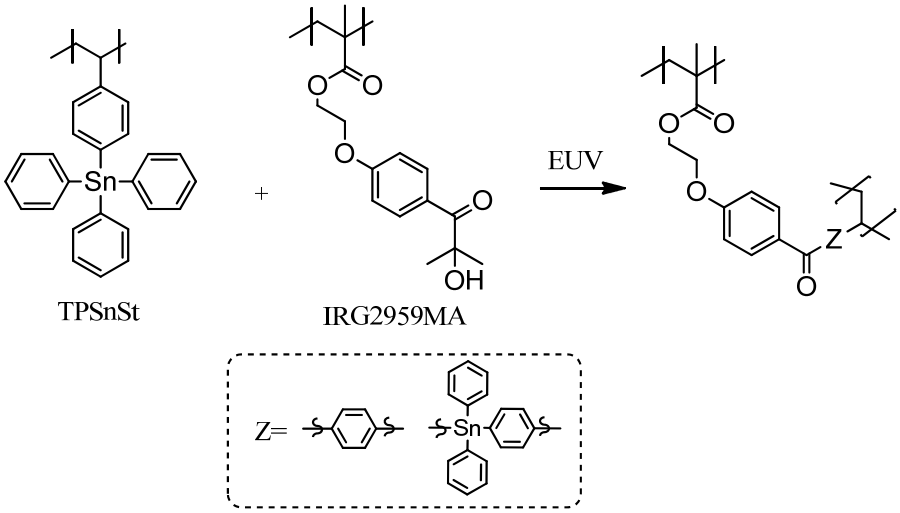

Fig. II-6 Presumed reaction process of crosslinking between TPSnSt and IRG2959MA.

2.3.4 Product analysis

Polymers II-5 and II-6 were analyzed by GPC after the exposure to EB to investigate the effect of TPSnSt on crosslinking. The GPC chromatograms of Polymers II-5 and II-6 are respectively shown in Figs. II-7 and II-8. The changes in the molecular weight and dispersity of Polymers II-5 and II-6 are shown in Tables II-9 and II-10, respectively. The rate of change of the molecular weight for Polymer II-5 was approximately twice that for Polymer II-6 at low EB exposure dose range from 20 to 60 μC/cm^2. The rate of change of the dispersion for Polymer II-5 was also higher than that for Polymer II-6. These results suggest radical generation from TPSnSt possibly through Sn-C bond scission. The additional radical generation is considered to

have contributed to the greater sensitivity enhancement than that expected from the increase in the EUV linear attenuation coefficient. The molecular weight of Polymer II-5 decreased above a dose region of >80 μC/cm^2, while the dispersions of Polymer II-5 at the exposure doses of 60, 80, and 100 μC/cm^2 were approximately the same. On the other hand, the molecular weight and dispersion for Polymer II-6 monotonically increased. Unbounded small radicals such as phenyl radicals and triaryl stannyl radicals generated from TPSnSt (Fig. II-5) may have suppressed the crosslinking between polymers when the concentration of unbounded small molecular radicals increased at high exposure doses.

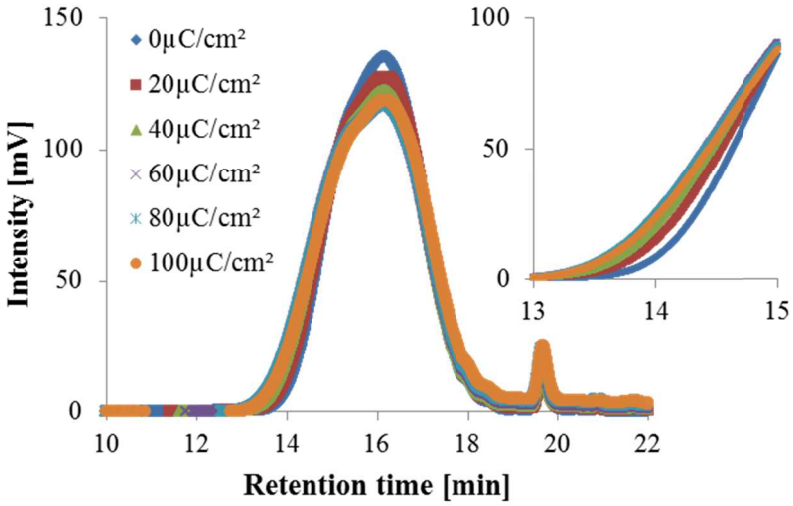

Fig. II-7 GPC chromatograms of Polymer II-5 exposed to EB. The inset is a magnified view. The horizontal and vertical axes represent the retention time in minutes and the intensity in mV, respectively. The numerical values next to μC/cm^2 represent the exposure doses.

Table II-9 Change in molecular weight upon exposure to EB

Sample	M_w					
	0 μC/cm^2	20 μC/cm^2	40 μC/cm^2	60 μC/cm^2	80 μC/cm^2	100 μC/cm^2
Polymer II-5	7409	8078	8604	9180	9149	8839
Polymer II-6	9335	9615	9919	10201	10479	10687

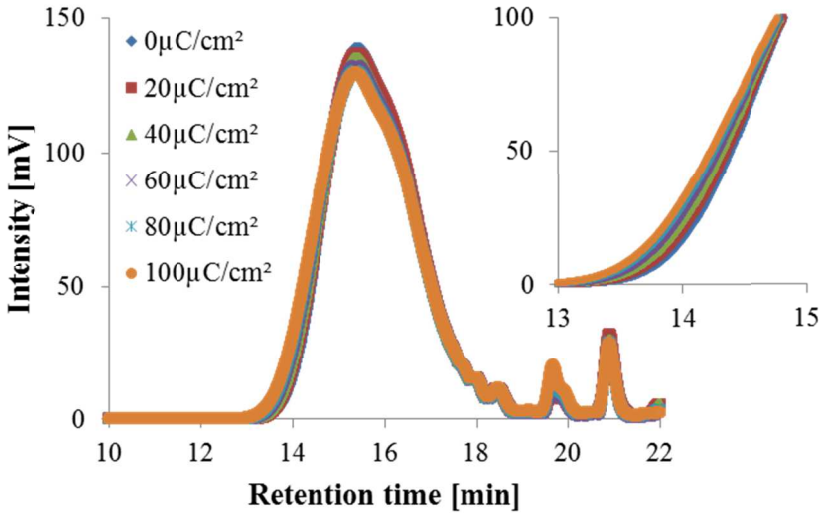

Fig. II-8 GPC chromatograms of Polymer II-6 exposed to EB. The inset is a magnified view. The horizontal and vertical axes represent the retention time in minutes and the intensity in mV, respectively. The numerical values next to μC/cm^2 represent the exposure doses.

Table II-10 Change in dispersity upon exposure to EB.

Sample	M_w/M_n					
	0 μC/cm^2	20 μC/cm^2	40 μC/cm^2	60 μC/cm^2	80 μC/cm^2	100 μC/cm^2
Polymer II-5	1.84	1.97	2.08	2.21	2.23	2.22
Polymer II-6	2.02	2.05	2.08	2.12	2.17	2.18

2.4. Conclusions

An organic tin compound with a large absorption cross section for 92.5 eV EUV radiation was introduced into dual insolubilization resists to improve their sensitivity. The synthesized resists were composed of triarylsulfonium cations as a polarity changer and radical generator, IRG2959MA as a radical generator, and TPSnSt as an EUV absorption enhancer. By the incorporation of TPSnSt, the linear attenuation coefficient of the polymer increased by approximately 30% and the sensitivity increased by more than two and a half times (the exposure dose for insolubilization was decreased by 60%). The additional sensitivity enhancement is considered to have been caused by the generation of polymer radical through Sn-C bond scission. Fluorine is known to be effective for enhancing of the EUV absorption of CARs. However, it has a negative effect on the decomposition of triarylsulfonium cations. In contrast, it was found that TPSnSt had no negative effect on the decomposition of triarylsulfonium cations.

2.5 References

1) T. Kozawa, J. J. Santillan, and T. Itani, Jpn. J. Appl. Phys. **52**, 076502 (2013).

2) T. Kozawa, J. J. Santillan, and T. Itani, Jpn. J. Appl. Phys. **55**, 096501 (2016).

3) D. D. Simone, V. Rutigliani, and G. Lorusso, et al. Proc. SPIE **10583**, 105830G (2018).

4) W. Montgomery, A. McClelland, and D. Ure, et al. Proc. SPIE **10143**, 1014328 (2018).

5) T. Kozawa, S. Tagawa, J. and J. Santillan, et al. J. Photopolym. Sci. Technol. **21**, 421 (2008).

6) T. Kozawa, H. Oizumi, and T. Itani, et al. Jpn. J. Appl. Phys. **49**, 036506 (2010).

7) J. Iwashita, T. Mimura, and T. Hirayama, et al. Proc. SPIE **7273**, 72733O (2009).

8) D. De Simone, S. Sayan, and S. Dei, et al. Proc. SPIE **9776**, 977606 (2016).

9) J. Stowers, J. Anderson, and B. Cardineau, et al. Proc. SPIE **9779**, 977904 (2016).

10) T. Kozawa, J. J. Santillan, and T. Itani, Jpn. J. Appl. Phys. **57**, 026501 (2018).

11) M. Krysak, M. Leeson, and E. Han, et al. Proc. SPIE **9422**, 942205 (2015).

12) J. Leebrick and H. Ramsden, J. Org. Chem. **23**, 935 (1958).

13) B. L. Henke, E. M. Gullikson, and J. C. Davis, At. Data Nucl. Data Tables **54**, 181 (1993).

14) N. Nomura, K. Okamoto, and H. Yamamoto, et al. Jpn. J. Appl. Phys. **54**, 06FE03 (2015).

15) R. N. Kapoor, P. Apodaca, and M. Montes, et al. Appl. Organomet. Chem. **19**, 518 (2005).

16) W. Uhlig, J. Organomet. Chem. **409**, 377 (1991).

17) K. Mochida, M. Wakasa, and Y. Sakaguchi, et al. Chem. Lett. 1793 (1986).

Chapter III

Incorporation of chemical amplification in dual insolubilization resist

3.1 Introduction

The maximum light source power which is the greatest concern in high-volume manufacturing (HVM) has markedly increased from tens of watt at intermediate focus (WIF) to hundreds of WIF.[1,2] The number of wafer tests has also dramatically increased using a high-power EUV light source.[3,4] The current development status suggests that the mass production using EUV lithography will be realized in the near future. Therefore, the current key issue is whether EUV lithography can be extended to sub-10 nm HP node. The greatest concern has shifted from the source power to the resist stochastic and RLS trade-off. Therefore, some ideas for improving the sensitivity and pattern uniformity of CARs have been studied with the aim of reducing the acid diffusion length of chemical reactions and increasing EUV absorption through the incorporation of high-EUV-absorption elements in CARs.[5,6] However, the acid diffusion length reduction of CARs are difficult unless the sensitivity is sacrificed by increasing the quencher concentration. The reaction rate of a deprotecting reaction and an acid scavenging reaction, which were mentioned in general introduction as described in scheme 1 (b-1), are determined by the concentrations. On the other hand, high-EUV-absorption dual insolubilization resists were realize an insolubilization property for developer with high sensitivity without utilizing any amplification reaction. Therefore, low diffusive acid catalytic reaction with high concentration scavenger is useful for additional sensitivity enhancement retaining low acid diffusion length.

In this study, to improve the sensitivity, an acid-catalytic reaction was applied to a high-EUV-absorption dual insolubilization resist consisting of PBC, PBRG, and PBSn as described in chapter 2. Diphenylmethanol derivatives are known to react readily with alcohols or to dimerize by an acid-catalytic reaction below room temperature to generate diphenyl or tetraphenyl ether derivatives [7,8] Also, aryl and alkyl stannic compounds are known to react readily with strong acids. TPSnSt did not affect the evaluation of acid generation using C6 in a chapter 2 because of the activation energy of neutralization being lower than that of stannylation. An organotin compound, however, has the potential to function as an acid quencher by competing with etherification since the activation energy of the etherifications of diphenylmethanol derivatives are not zero. Applying organotin compounds as an acid quencher is expected to be superior to alkylamine-type quenchers from the viewpoint of EUV absorptivity, resist film density, and etching resistance. The diphenylmethanol derivative used as a polymer-bound acid reactivity unit was 4-[(2,4-dimethoxyphenyl)hydroxymethyl]phenylmethacrylate (ARMA). The effects of the

chemical amplification on the sensitivity and the acid quenching effect of TPSnSt were investigated.

3.2 Experimental methods

3.2.1 Materials

MAPDPS-MSA, MAPBpS-MSA, and TPSnSt were prepared as described in section 1.2.1. and 2.2.1. ARMA was synthesized in accordance with a conventional esterification reaction. Polymers were synthesized and analyzed by same procedure described in section 1.2.1. except that. α-Thioglycerol was applied as a chain transfer agent to synthesize Polymer III-2, which is a low weight-average molecular weight (M_w) version of Polymer III-1. The concentration of α-thioglycerol was adjusted to 9 mol% of the total molar number of monomers. The details of polymer properties are shown in Table III-1. The molecular structures of the monomers are shown in Fig. III-1.

Molecular weights were determined by GPC analysis same as described in section 2.2.1. The molecular weights determined using polystyrene standards are also listed in Table III-1. Note that the composition ratios in Table III-1 are expressed in mol%.

Table III-1 Composition ratios of monomer units and polymer properties.

Sample	Composition ratio (mol%)						Molecular weight (Mw)
	MAPDPS-MSA	ARMA	TPSnSt	IRG2959 MA	HAMA	PhMA	
Polymer III-1	25	23	32	20			101300
Polymer III-2	27	23	30	20			13100
Polymer III-3	24		56	20			35500
Polymer III-4	29			27	22	22	5000

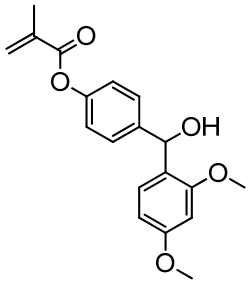

ARMA

Fig. III-1 Molecular structures of ARMA.

3.2.2 Sensitivity (E_0) evaluation

The sensitivity evaluation samples and developers for each polymer were prepared by the same procedure as described in Section 1.2.2. Selected developers as the developer for each polymer were shown in Table III-2 except that HMDS treatment was omitted for the resist samples of Polymers III-1 and III-2 because they were highly adhesive to wafer without HMDS treatment.

The resist films were exposed to by the same procedure described in Section 1.2.2. The exposure dose range was applied from 0.25 to 2.5 mJ/cm^2 in this experiment.

Table III-2 Acetonitrile concentration in developer, optimized for each polymer.

Sample	Acetonitrile concentration [vol%]
Polymer III-1	30.0
Polymer III-2	30.0
Polymer III-3	37.5
Polymer III-4	20.0

3.2.3 Acid generation efficiency evaluation by EUV irradiation

The evaluation samples for acid generation efficiency were prepared by the same procedure as described in Section 1.2.3. The film thicknesses were 553, 675, and 635 nm for Polymers III-2, III-3, and III-4, respectively. The samples were exposed to EUV radiation with a dose from 3 to 9 mJ/cm^2. Then, the acid yields were measured the same procedure as described section 1.2.2.

3.2.4 EB patterning

The samples of Polymers III-2-III-4 used for evaluation were prepared with the same procedure as that described in Section 1.2.3, except that the weight ratio of polymer to solvent was 1:30. The resist films with a thickness of 50 nm were obtained after spin-coating process.

The resist films were exposed to EB radiation from a 125 keV EB exposure system (Elionix ELS-F100T) with a dose from 20 to 300 μC/cm^2. After the EB exposure, the resist films were developed with the developer for 30 s at 25 °C and rinsed with deionized water for 30 sec. The delineated patterns were observed by scanning electron microscopy (SEM) (Hitachi High-Tec. S-5500). The pitch of the line-and-space patterns was 160 nm. The exposure pattern width of the lines was 25 nm. The SEM images were analyzed using line edge roughness (LER) measurement software, which measures the mean LER of an entire image.[9] Samples of

Polymer III-2 with 10 and 20 wt% trioctylamine (TOA) relative to the PBC content of the polymer were also prepared to examine the acid quenching efficiency of TPSnSt.

3.3 Results and discussion

3.3.1 Sensitivity (E_0) evaluation

Fig. III-2 shows the relationship between the EUV exposure dose and the normalized residual film thickness after rinsing for Polymers III-1 to III-4. Note that the necessity and validity of optimizing the developer for each polymer used for the sensitivity evaluation have been described in chapter 1. The sensitivity (E_0) was evaluated to be 0.25, 0.25, 0.6, and 0.9 mJ/cm^2 for Polymers III-1, III-2, III-3, and III-4, respectively. The sensitivities of the ARMA-containing polymers were higher than that of Polymer III-3, which did not contain ARMA. Diphenyl methanol derivatives are well known to generate ethers by an acid-catalyzed reaction with alcohols, including dimerization. Since the reactivity of diphenyl methanol derivatives with tertiary alcohols is lower than that of the dimerization, generally, dimerized products are mainly generated in solution. However, under aggregating conditions such as film or bulk conditions, the diffusion of components is significantly restricted, particularly for a polymer-bound condition. Therefore, the etherification with IRG2959MA is considered to also be possible in the resist film, as shown in Fig. III-3. IRG2959MA is considered to contribute to the insolubilization of the resist in the developer through the radical and acid-catalytic cross-linking, as discussed in the following sections. For Polymers III-1 and III-2, the sensitivities were approximately the same. However, Polymer III-2 swelled particularly at low doses, as shown in Fig. III-2. Generally, a high-M_w polymer tends to swell more than a low-M_w polymer. The reason for the swelling of Polymer III-2 (low M_w) is considered to be related to the difference in the synthesis. In the synthesis of Polymer III-2, α-thioglycerol was applied as a chain transfer agent. It can attach to the polymer head and tail through the radical state and a sulfide can be formed at the polymer chain ends. The polymer bound sulfide is considered to have increased the acetonitrile concentration of the developer, enabling its complete dissolution of the polymer due to its hydrophobicity and low dielectric constant. We synthesized a polymer with a lower M_w than Polymer III-2 by increasing the amount of α-thioglycerol twofold. The acetonitrile concentration of the developer required for complete dissolution was 45% even though the M_w of the synthesized polymer was only 4300. For the reason given above, Polymer III-2 exposed to a low dose is considered to be susceptible to swelling during development owing to a low crosslinking density and a small change in polarity compared with those at high doses. A low-M_w polymer is necessary for the fabrication of patterns with high resolution and low LWR.

A method of reducing M_w without increasing the hydrophobicity is required to improve the properties of the chemically amplified dual insolubilization resist for application to the high-resolution patterning.

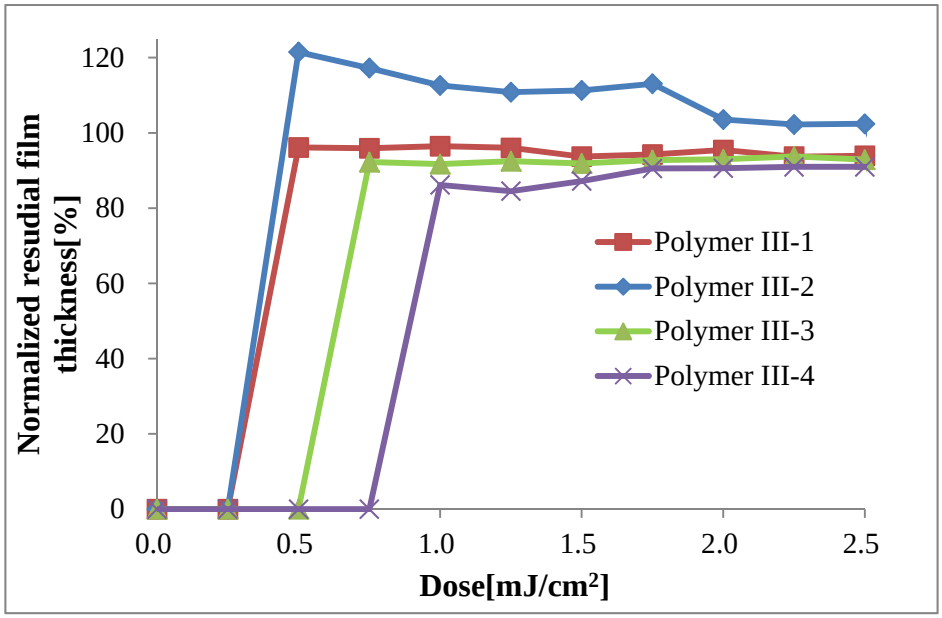

Fig. III-2 Sensitivity curves of Polymers III-1-III-4 upon exposure to EUV radiation.

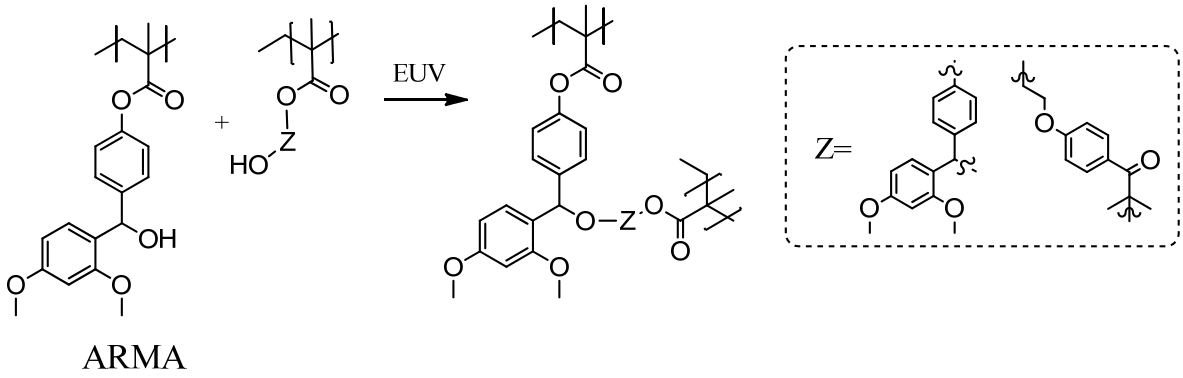

ARMA

Fig. III-3 Presumed reaction between ARMA and IRG2959MA and dimerization.

3.3.2 Acid generation efficiencies

The acid yields of Polymers III-2-III-4 were determined by the UV-VIS spectrophotometric determination of protonated C6 absorption to investigate the decomposition of PBC units. After exposure to EUV radiation, an absorption band appeared at 533 nm. This indicated that C6 became protonated C6. The absorption intensity is plotted against the exposure dose in Fig. III-4. The absorption intensity was normalized with the film thickness. The acid generation efficiencies were evaluated from the slopes of the graphs by taking into account the differences

in film thickness and linear attenuation coefficient. Table III-3 shows the relative acid generation efficiency for EUV irradiation. The acid generation efficiencies were normalized with that of Polymer III-4. Although the acid generation efficiencies of Polymers III-2 and III-3 were lower than that of Polymer III-4, the sensitivities of Polymers III-2 and III-3 were 3.6 and 1.5 times higher than that of Polymer III-4, respectively. As descried in chapter 2, the sensitivity of a PBSn-containing dual insolubilization resist was 2.5 times higher than that of the dual insolubilization resist without PBSn owing to the increase in cross-linking efficiency due to the Sn-C bond scission for approximately the same PBC concentrations of these resists. The sensitivity of Polymer III-3 was still 1.5 times higher than that of Polymer III-4 upon EUV exposure even though the PBC concentration (per unit volume) of Polymer III-3 was two-thirds that of Polymer III-4. Note that the composition ratios in Table III-1 are expressed in mol%. Polymer III-2 showed the highest sensitivity among Polymers III-2-III-4 despite its lower acid generation efficiency than Polymer III-4 and its lower PBSn content than Polymer III-3. This increased sensitivity is considered to be due to the reactivity of ARMA in the presence of the acid catalyst. The high sensitivity despite the low acid generation efficiency also supports the assumption that IRG2959MA contributes to the etherification. This assumption is further examined on the basis of patterning results in the next section.

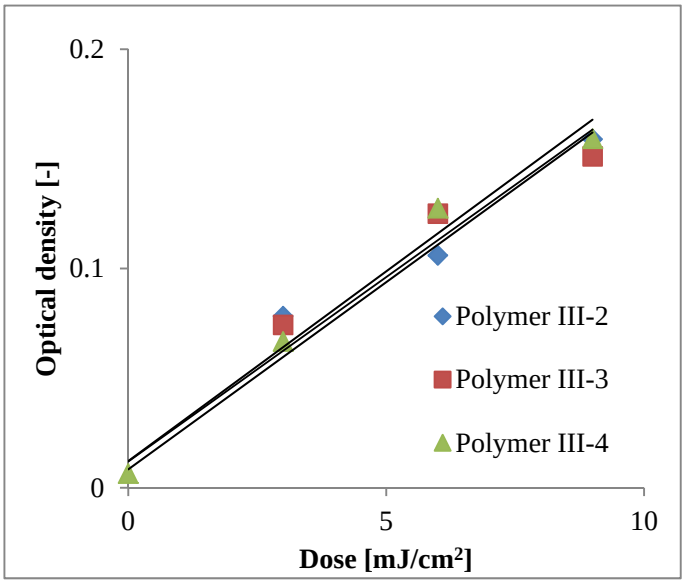

Fig. III-4 Dependence of optical density of protonated C6 on EUV exposure dose.

Table III-3 Relative acid generation efficiency upon exposure to EUV radiation and linear attenuation coefficient μ of EUV (92.5 eV).

Sample	Relative acid generation efficiency*	μ [/μm]
Polymer III-2	0.82	5.41
Polymer III-3	0.90	5.64
Polymer III-4	1.00	4.63

3.3.3 EB patterning

The EB patterning results for Polymers III-2-III-4 are shown in Fig. III-5. The exposure pattern width and pitch were 25 and 160 nm, respectively. For the pitch of 50 nm, the resist patterns were not obtained. The sensitivity of Polymer III-3 was only 20% higher than that of Polymer III-4 even though the sensitivity of the 1×1cm^2 pattern upon EUV radiation was 1.5 times higher than that of Polymer III-4. The line width and LER of Polymer III-3 were 1.5 and 1.9 times thicker than those of Polymer III-4, respectively. The reason for the performance deterioration of Polymer III-3 (in comparison with Polymer III-4) is considered to be the poor adhesion of Polymer III-3 due to the high composition ratio of TPSnSt, which is a low-polarity compound. Polymers with poor adhesion are easily peeled away from the wafer surface or induce pattern collapse during development. The excess exposure to obtain sufficient adhesion is considered to have increased the line width. The sensitivity of Polymer III-2 was more than three times that of Polymer III-4. This high sensitivity supports the assumption that IRG2959MA contributes to the etherification. However, the line pattern of Polymer III-2 was jagged. This result suggests that the acid quenching of TPSnSt was insufficient to suppress the acid diffusion, which is a cause of LER.[10)]

Fig. III-5 SEM images of line-and-space patterns fabricated with Polymers III-2-III-4. The exposure pattern width was 25 nm and the pitch was 160 nm.

The EB patterning of Polymer III-2 with TOA was carried out to examine the acid quenching efficiency of TPSnSt, as shown in Fig. III-6. When the acetonitrile concentration of the developer was 30%, the line width and LER of Polymer III-2 without TOA were 58 and 12.9 nm at 120 μC/cm^2, respectively. The minimum dose required for the formation of the line patterns of Polymer III-2 without TOA was 60 μC/cm^2 and the line width and LER were 43.7 and 15.3 nm, respectively. Upon the addition of 10 wt% TOA to the PBC content of Polymer III-2, the line width and LER of Polymer III-2 became 47.8 and 10.4 nm, respectively, at 120 μC/cm^2, which was the minimum dose required for the line formation of this sample. This dose was excessive for Polymer III-2 without TOA. The line width became narrow and LER became small upon the addition of TOA. This indicates that the pattern formation reaction can be terminated by the addition of quenchers. TPSnSt seemed to lack the ability to quench acids required for the etherification of ARMA. In the case of 20 wt% TOA addition, many scums were observed for the developer with 30 vol% acetonitrile. This is considered to be caused by the hydrophobized effect of the long-chain alkyl amine. The fact that the acetonitrile concentration was adjusted to be close to the dissolution threshold is likely to have affected the patterning results. The developer with 35 vol% acetonitrile was examined to investigate the effect of the quencher. SEM images are shown in the lower row of Fig. III-6. For all the samples, the line width and LER were approximately the same, regardless of the TOA concentration. Therefore, TPSnSt is considered to have also acted as a quencher, although its quenching ability was lower than that of TOA. This agrees with the result in chapter 2 that TPSnSt did not affect the reaction of C6 (a strong quencher with quenching ability comparable to TOA) with acids. For the developer with 30 vol% acetonitrile, the difference in quenching ability is considered to have affected the line width and LER, because the solubility of the developer was set to be near the threshold of the unexposed resist.

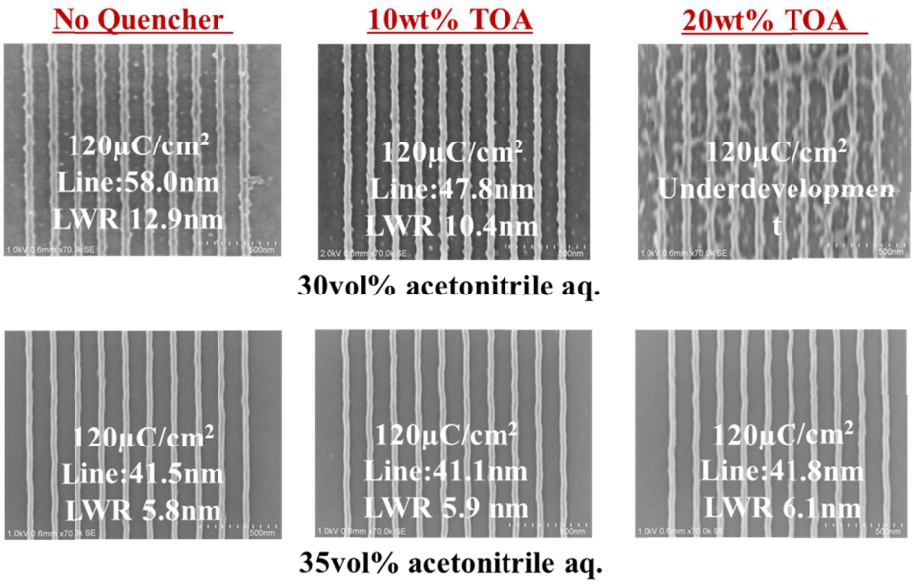

Fig. III-6 Effects of TOA on line-and-space patterns fabricated with Polymer III-2. The exposure pattern width was 25 nm and the pitch was 160 nm.

On the basis of the discussion previously described, a low-M_w version of Polymer III-2 (Polymer III-5) was synthesized using a different chain transfer agent and a solvent not to increase the minimum concentration of acetonitrile required for the complete dissolution of the unexposed polymer, namely, not to significantly increase the hydrophobicity of the polymer. The composition ratio and the properties of Polymer III-2 and III-5 are shown in Table III-5. M_w of Polymer III-5 was 6300. The minimum concentration of acetonitrile was the same as those of Polymers III-1 and III-2 (30.0 vol%). Using Polymer III-5, the line-and-space patterns were fabricated. The resist sample for the patterning was prepared through the same procedure described in Section. 3.2.4. The acetonitrile concentration in developer was slightly increased to 35 vol% to avoid the generation of scums, as described previously for Polymer III-2.

Table III-5 Composition ratio of monomer units and polymer properties.

Sample	Composition ratio (mol%)				Molecular weight (Mw)	Developer concentration (Acetonitrile vol%)
	MAPDPS-MSA	ARMA	TPSnSt	IRG2959 MA		
Polymer III-2	27	23	30	20	13100	30.0
Polymer III-5	25	24	32	19	6300	30.0

Figure III-7 shows the line-and-space patterns with 25 nm half-pitch, fabricated using Polymer III-5. LWR was 2.1 nm. The resolution and LWR were significantly improved, compared with Polymers III-3 and III-4 (also, compared with Polymer III-2). The sensitivity was 160 μC/cm^2 at the electron beam energy of 125 keV, which corresponds to approximately 90 μC/cm^2 at the electron beam energy of 50 keV (the beam energy of typical mask writers). As is well known as the trade-off relationship between resolution and sensitivity, the sensitivity decreased with the increase of resolution. For the 25 nm line-and-space patterns of chemically amplified resists, the sensitivity of 100 μC/cm^2 at the beam energy of 50 keV is regarded as a high sensitivity.[12)] Polymer III-5 showed the sensitivity comparable to the high-resolution chemically amplified EB resists. The improvement of resist performance can be expected by further reducing M_w without increasing hydrophobicity.

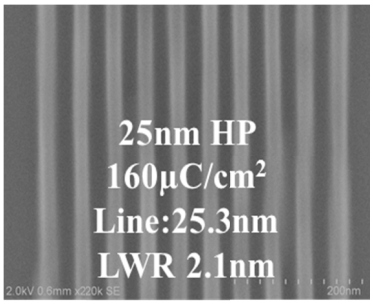

Fig. III-7 SEM images of 25nm line-and-space half pitch patterns fabricated with Polymer III-5

3.4 Conclusion

An acid-reactive compound was introduced into organotin-containing dual insolubilization resists to improve their sensitivity. The synthesized resists were composed of triarylsulfonium cations as a polarity changer and a radical generator; 2-hydroxy-2-methylpropiophenone as a radical generator; TPSnSt as an EUV absorption enhancer; and ARMA as a polymer-bound acid-reactive unit. By the incorporation of ARMA, the sensitivity of EUV irradiation was increased 2.4-fold from 0.6 mJ/cm^2 of Polymer III-3 to 0.25 mJ/cm^2 of Polymer III-2 (the exposure dose required for insolubilization was decreased by approximately 60%). The increased sensitivity is considered to have been caused by the acid-catalytic etherification of ARMA through dimerization and/or with IRG2959MA. TPSnSt had a sufficient acid quenching capability for the acid-catalytic etherification. In the 125 keV EB patterning, the organotin-containing dual insolubilization resist with ARMA showed 25 nm half-pitch resolution with 2.1 nm LWR at the sensitivity of 160 μC/cm^2 (approximately 90 μC/cm^2 for 50 keV EB). The further improvement of resist performance can be expected by reducing M_w without increasing hydrophobicity.

3.5 References

1) Y. Ueno, T. Hori, and Y. Kawasuji, et al. Proc. SPIE **10583**, 1058328 (2018).

2) H. Mizoguchi, H. Nakarai, and T. Abe, et al. Proc. SPIE **10583**, 1058318 (2018).

3) R. V. Es, M. V. Kerkhof, A. Minnaert, and G. Fisser, et al. Proc. SPIE **10583**, 105830H (2018).

4) M. Purvis, I. V. Fomenkov, A. and A. Schafgans, et al. Proc. SPIE **10583**, 1058327 (2018).

5) Y. Vesters, J. Jiang, and H. Yamamoto, et al. Proc. SPIE **10583**, 1058307 (2018).

6) H. Furutani, M. Shirakawa, and W. Nihashi, et al. Proc. SPIE **10583**, 105860G (2018).

7) C. M. Welch and H. A. Smith, J. Am. Chem. Soc. **72**, 4748 (1950).

8) F. Toda and K. Okuda, J. Chem. Soc., Chem. Commun. **17**, 1212 (1991).

9) https://lacerm.com/

10) T. Kozawa and S. Tagawa, Jpn. J. Appl. Phys. **49**, 030001 (2010).

11) H. Tsubaki, S. Tarutani, and N. Inoue, Proc. SPIE **9051** 90511J-1 (2014)

12) T. Kozawa, Jpn. J. Appl. Phys. **55**, 056503 (2016).

Conclusion

I developed a negative type polymer resist with a high sensitivity. In the developed resist, two decomposition reactions (PBC and PBRG) were induced. PBCs showed high polarity conversion efficiency by generating an aryl sulfide from sulfonium salt and a radical simultaneously by dissociative electron attachment and electron excitation. PBRG generated radicals through the electronic excitation upon EUV irradiation. The two radicals generated from PBC and PBRG were considered to react with each other by the radical recombination from the result of EUV sensitivity curves. These two reactions are highly effective reactions for insolubilization to developer. The dissolution contrast was obtained with high sensitivity without a chemically amplified reaction. Therefore, this resist was named as a highly sensitive dual insolubilization EUV resist. Furthermore, the decomposition ratios of PBCs were evaluated for the dissociative electron attachment and electron excitation process, on the basis of the different decomposability of MAPDPS-MSA and MAPBpS-MSA observed by the acid generation efficiency evaluation and decomposition product analysis of 75 keV EB irradiation. Contrary to the expectation from the results of CARs, these results indicated that the electron excitation process have an advantage over the dissociative electron attachment when the PBC composition ratio in the resist is significantly higher than the conventional CARs which are generally contained 10-20 wt% PAG of the total weight of resist. (Chapter I)

Secondary, I developed an organometallic-compound-containing dual insolubilization EUV resist using TPSnSt, which contain a tin known as a high EUV absorption atom. The developed resist showed the 30 % increase of EUV absorption coefficient and 2.5 times higher sensitivity, compared with the polymers without TPSnSt. TPSnSt increased the acid generation efficiency through the increase of secondary electron generation due to the improvement of EUV absorption. In addition to the increase of EUV absorption, a radical was generated by cleavage of Sn-C bond of the structure. Although the absorption enhancement is taken into account, the increase of the radical recombination efficiency was considered to greatly contribute to the sensitivity improvement of the resist. From the evaluation of the acid generation efficiency of the polymer, TPSnSt did not show any negative effects that decrease the decomposition efficiency of sulfonium and the acid generation efficiency unlike a fluorine compound having a large EUV absorption coefficient. (Chapter II)

To increase the sensitivity of the resist as described in Chapter II, I incorporated ARMA, which is an acid reactive monomer, to introduce an acid catalyst crosslinking reaction, focusing on the strong acid generated by the PBC decomposition. ARMA was effective for increasing

sensitivity. Furthermore, nearly identical patterning results were obtained for the resists with and without trioctylamine which is used as an acid diffusion control agent. For obtaining a high-resolution line and space pattern, a low molecular weight polymer was synthesized and patterned using an EB writer. As a result, 25 nm line and space with 2.1 nm LWR was obtained. This resist was capable of high sensitivity patterning although it contained the high concentration of acid reactive organo-tin compound acting as an acid quencher. The etching resistance of the resist is expected to be higher than conventional CARs due to the high etching resistance of tin. Even if the resist is thinned for the high resolution patterning, a resist having high etching resistance can maintain a role as a resist for selective etching of silicon substrate. A low LWR feature is advantageous to obtain a high-definition pattern less than 15 nm or less. These features of the chemically amplified dual insolubilization resists are expected to have advantages for sub 15nm resolution patterning with good sensitivity and low LWR. (Chapter III)

List of publication

1. Study of electron-beam and extreme-ultraviolet resist utilizing polarity change and radical crosslinking
   Satoshi Enomoto, and Takahiro Kozawa
   Journal of Vacuum Science & Technology B 36, 031601 (2018).

2. Effects of organotin compound on radiation-induced reactions of extreme-ultraviolet resist utilizing polarity change and radical crosslinking
   Satoshi Enomoto, Takumi Yoshino, Kohei Machida, and Takahiro Kozawa
   Japanese Journal of Applied Physics 58, 016504 (2019).

3. Incorporation of chemical amplification to dual insolubilization resist
   Satoshi Enomoto, Takumi Yoshino, Kohei Machida, and Takahiro Kozawa
   Japanese Journal of Applied Physics, in press.

Acknowledgement

This study has been carried out under the guidance of Professor Takahiro Kozawa at the Department of Beam Material Science, the Institute of Scientific and Industrial Research Osaka University. I would like to express my grateful gratitude to Professor Takahiro Kozawa for the continuous support and many insightful advices for my research. The knowledge gained from discussion and guidance corrected the direction of my research. In addition, the knowledge and experience obtained from this doctoral program are tremendous assets for future research activities. I look forward to continuous guidance from Professor Kozawa as one of the leaders in our research field.

I would like to also express my gratitude to Professor Susumu Kuwabata and Professor Masaya Nogi for the invaluable scientific advices from different fields of specialists.

I would like to express my gratitude to former Assistant Professor Hiroki Yamamoto for teaching about indispensable experimental equipment for research activities. I am very pleased to hear that he is doing fine in QST. Please continue to have a good relationship.

I would like to express my gratitude to the staff member of Kozawa Lab., Associate Professor Yusa Muroya, Assistant Professor Kazumasa Okamoto, Specially Appointed Professor Kazuo Kobayashi, Specially Appointed Assistant Professor Ayako Nakajima and Ms. Kinuko Watanabe for supporting my research. I will bring souvenir of eastern Japan when I come in near here even after graduation.

I would also like to thank Dr, Tsuneishi, Mr. Konda, Mr. Kanamori, Ms. Tsutsui, Mr. Ishihara, Mr. Tanaka, Ms. Kariya, Mr. Yamada, Mr. Ikari, and Mr. Maeda who were always studying diligently while I was studying in Kozawa Lab. I think that a bright future is waiting for all of them who do not forget diligence.

I would like to express my gratitude to Dr. DINH Cong Que, who is a friend of mine, for providing Lacerm program which is useful pattern width measurement software and for teaching about SEM. I have always learned and encouraged from his behavior and effort in Japan. I am very pleased to hear that he is doing fine in a Japanese company. Please continue to have a good relationship.

I would like to express my gratitude to the research group members of Toyogosei Co., Ltd. Yusuke Suga, Takumi Yoshino, Kohei Machida, Michiya Naito, who had supported the compatibility between study and work for three years. I have been fortunate to have dependable colleagues who are able to get the result during my absence.

I would like to express my gratitude to President Yujin Kimura, Dr. Takashi Miyazawa, and Dr. Yasushi Mori who are the board members and auditor of Toyogosei Co., Ltd. for supporting me to attend this doctoral course. The presence of an understanding boss in research activities is very encouraging to us.

I would like to express my great gratitude to Honorary President Masateru Kimura of Toyogosei Co., Ltd. In addition to encouraging enrollment of the course for getting a doctorate this time, he also gave me numerous guidance and invaluable advices since joining the company. His curiosity and faculty that never wane beyond the eighty-five always encouraged and directed me to research activities. I believe that the foundation founded in his spirit of social contribution after retiring the company supports many young researchers and students, and contributes to the development of science. I wish his long-lasting good health.

I have been very grateful to my wife who accepted and supported my challenges at a very hard time and my mother who raised two brothers and me with single parenthood. I owe what I am to my family. I also thank my son who always greeted me with a smile even though I left the house for a long time nearly every month. I am happy if I can support him to meet wonderful teachers like me in his future.